TABLE 2. Grading: necroinflammatory scores and fibrosis

Group	Inoculum	Tupaia no.	Grade				Total	Avg	SD	Staging
			A	B	C	D				
94 wk p.i. (biopsy)										
I	HCR 6	Tup.5	0	0	0	0	0	1.3	1.5	0
		Tup.6	1	0	1	0	2			0
	RCV	Tup.4	0	0	0	0	0			0
		Tup.8	0	0	0	3	3			6
	Control	Tup.15	0	0	0	0	0	0	0	0
III		Tup.17	0	0	0	0	0			0
		Tup.38								
		Tup.39								
144 wk p.i. (sacrifice)										
I	HCR 6	Tup.5	1	0	2	3	6	5.5	3.7	0
		Tup.6	3	0	4	3	10			1
	RCV	Tup.4	0	0	0	1	1			0
		Tup.8	1	0	1	3	5			6
	Control	Tup.15						0	0	
III		Tup.17								
		Tup.38	0	0	0	0	0			0
		Tup.39	0	0	0	0	0			0

defined genotype (genotype 1b), and genetic heterogeneity was ascertained by the process of cloning consensus cDNA. The infectivity of this serum was also experimentally defined in chimpanzees; a 50% chimpanzee infectious dose was estimated at 3.7×10^4 50% chimpanzee infectious doses/ml. Furthermore, the consensus genomic sequence of HCV was cloned from the serum (pHCR6; 9,611 bases; GenBank AY045702.1). For the second inoculum (referred to as RCV), clonal viral particles were reconstituted as described in Materials and Methods. This inoculum was expected to be free of neutralizing antibodies and thus was considered potentially more infectious than patient sera. In the case of RCV infection, genetic diversification of viral RNA, also known as quasispecies, can be regarded as a direct indication of de novo synthesis of progenitor virus in vivo.

Either patient serum or cDNA-derived RCV was inoculated into tupaias (Table 1, group I). Two animals (one female and one male) were tested against each inoculum. Age-matched animals were bred as infection-free controls.

All experimental infections are described in Materials and Methods and Table 1. Prior to experimental infection, the normal serum ALT level in tupaias was measured at 22.3 IU/liter ($n = 23$).

Inoculation with patient serum HCR6 caused rapid fluctuations in the serum ALT concentrations, from two- to fivefold, in both inoculated tupaias, suggesting acute hepatitis in vivo (Fig. 1A and B). Correlative quantitative RTD-PCR revealed HCV viremia soon after serum inoculation in Tup.5, which continued to show transient viremia long term. The appearance of viremia sometimes coincided with a steep elevation in the serum ALT (Fig. 1A). Conversely, HCV RNA was not detected in the serum of Tup.6 up to 60 weeks postinoculation and only twice thereafter. Acute-phase ALT elevations (3 to 4 weeks postinoculation) in Tup.6 might represent tight control of HCV infection by the host immune system (Fig. 1B).

Distinct results were obtained for the two animals (Tup.4 and Tup.8) inoculated with RCV. Both animals displayed sustained viremia up to 10 weeks postinoculation (Fig. 1C and D), indicating persistent HCV infection and inability to eradicate the virus. Viremia was detected intermittently throughout the course of infection, sometimes accompanying the elevation of serum ALT. Humoral immune responses in Tup.5 and Tup.6 (see Fig. S1A in the supplemental material) and Tup.4 and Tup.6 (see Fig. S1B in the supplemental material) were indicated.

We performed RTD-PCR to confirm whether HCV could replicate in the tupaias' livers (Tup.4, Tup.5, Tup.6, and Tup.8) and obtained the following results (Fig. 1E): 310 ± 117 copies/μg total RNA in Tup.5, 80 ± 11 copies/μg in Tup.6, 199 ± 77 copies/μg in Tup.4, and 292 ± 48 copies/μg in Tup.8. In contrast, HCV RNA was not detected in the liver of the mock-infected animal (Tup.15).

HCV RNA was also not detected in samples from either preinoculation or age-matched, infection-free control tupaias (Table 1, group III), nor were significant elevations in serum ALT observed for any of the three infection-free controls (data not shown).

HCV causes chronic hepatitis in tupaia liver, leading to fibrosis and cirrhosis. Serum ALT and circulating HCV RNA levels in primary infected tupaias (Table 1, group I) were monitored for 3 years postinoculation. As described above, the magnitudes of serum ALT fluctuations varied substantially among infected animals (Fig. 1A, B, C, and D). Tupaia livers were examined for histological lesions in order to elucidate if HCV caused chronic hepatitis. Liver biopsies via abdominal incisions were performed at 2 years postinoculation. All animals were sacrificed at 3 years postinoculation (4.5 years for uninfected animals). H&E staining of liver specimens from HCV-infected tupaias showed infiltrating lymphocytes within sinusoids and around portal areas, indicating chronic hepatitis in the tupaia livers (Fig. 2B, D, and H). Infiltrating lymphocytes were also observed in limiting plates, indicating ongoing inflammation (Fig. 2G and H). Furthermore, a comparison of liver samples at 2 and 3 years postinoculation revealed that the

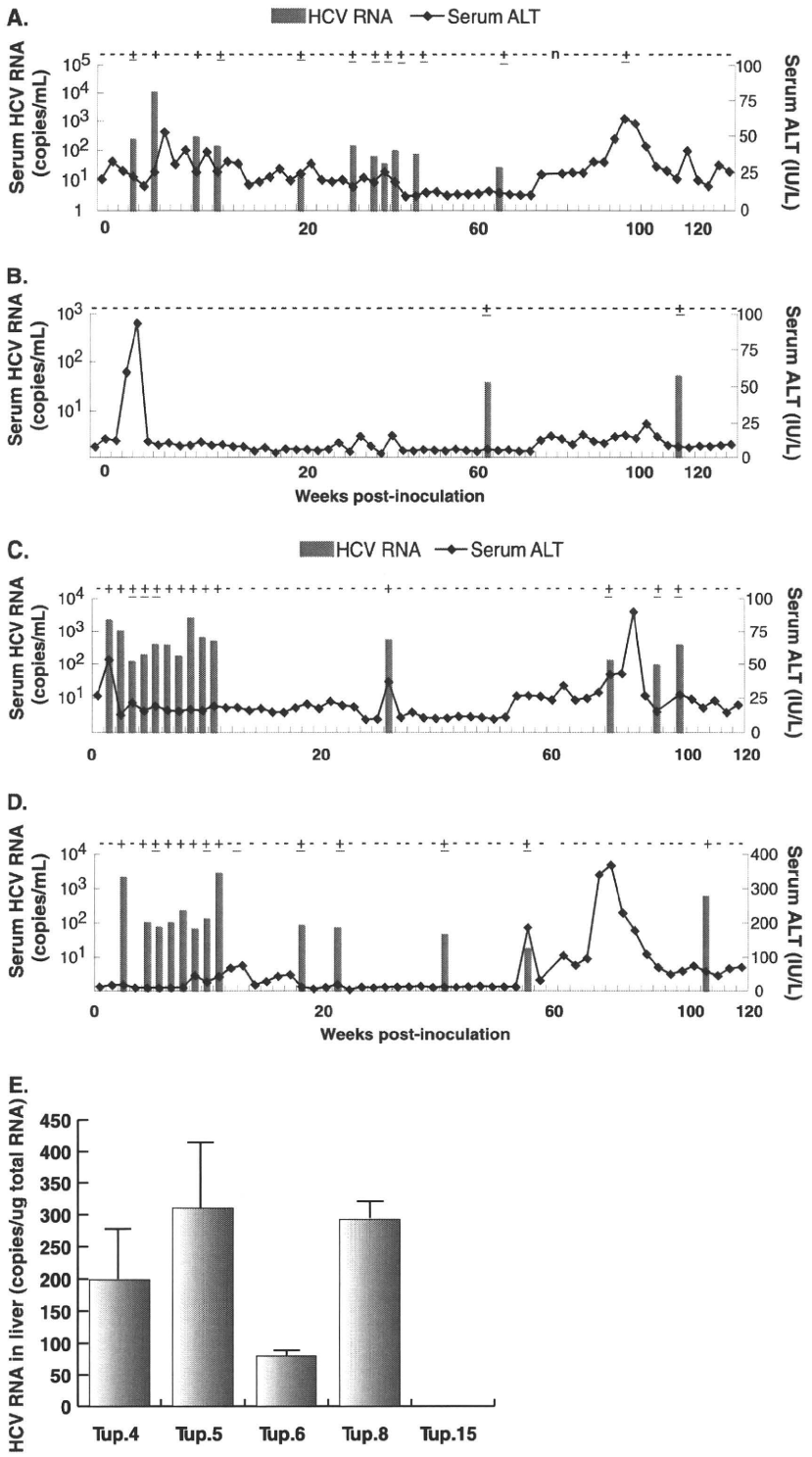

FIG. 1. Course of infection with patient serum HCR6 and RCV. (A) The results of quantitative RTD-PCR for HCV RNA and serum ALT concentrations were combined and plotted to show the course of infection in Tup.5. The bars and the ordinates on the left represent HCV RNA as genome equivalents/ml of serum. The curved line and the ordinates on the right represent serum ALT concentrations as IU/liter serum. (B) Serum HCV RNA and ALT concentrations for infection of Tup.6. (C) The graph for Tup.4. (D) The graph for Tup.8. The vertical axis for serum ALT in this graph is scaled differently from the others because of significant ALT elevation. (E) Quantification of HCV RNA in tupaia liver. HCV RNA in hepatocytes from tupaia (Tup.4, Tup.5, Tup.6, Tup.8, and Tup.15) livers was isolated 172 weeks after HCV infection and quantified by RTD-PCR. As few as 10 copies of the genome were detected, and the quantification range was between 10^1 and 10^8 copies (26).

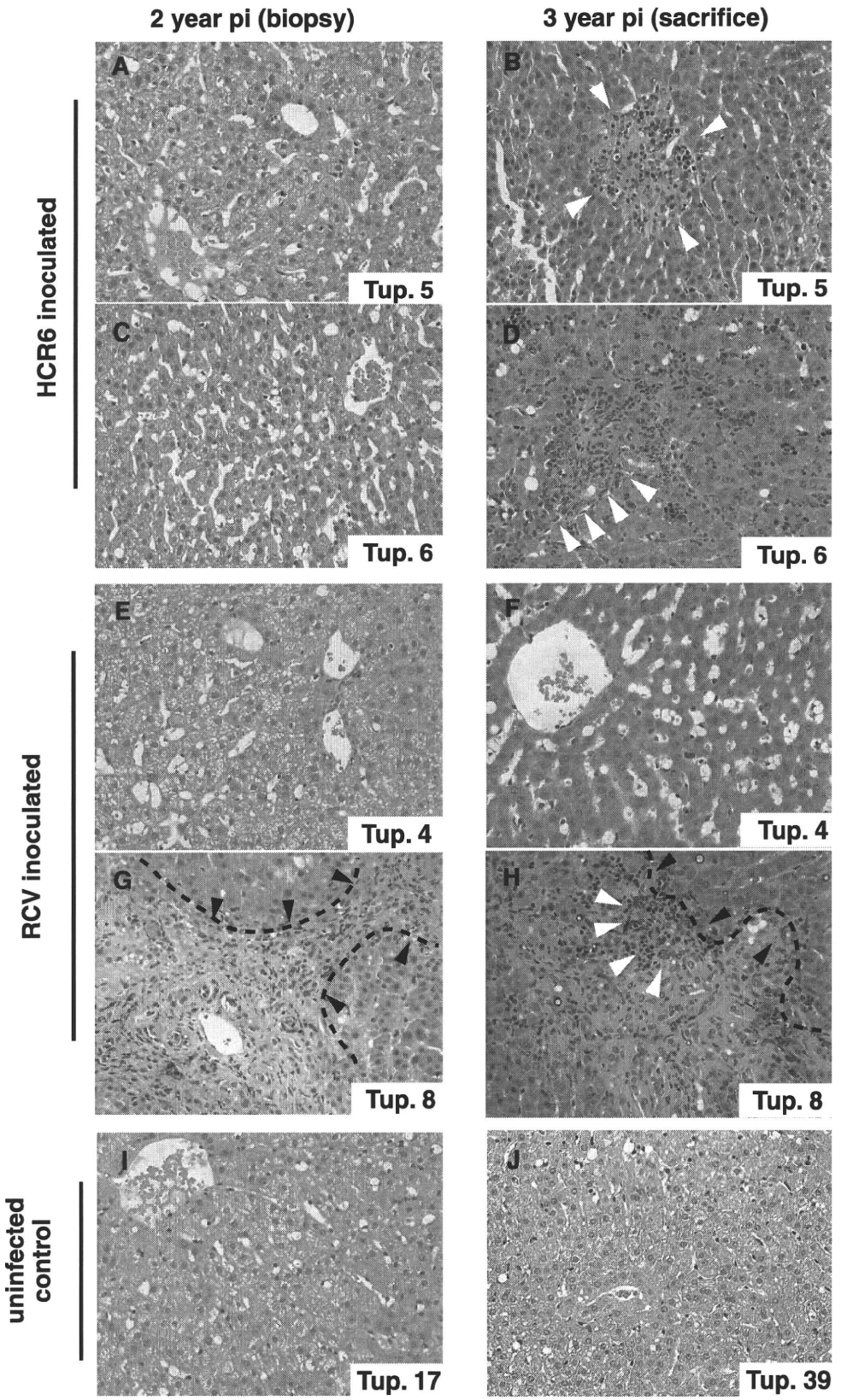

FIG. 2. Micrographs of liver specimens stained with H&E. Liver tissue from HCR6-inoculated tupaias (A to D) and RCV-inoculated tupaias (E to H) was obtained at 2 and 3 years postinoculation (pi). (I and J) Liver specimens from uninfected animals age matched to each inoculated animal were also obtained. The HCV-infected tupaia livers harbored infiltrating lymphocytes (white arrowheads) and fibrosis (broken lines and black arrowheads), which indicate chronic hepatitis.

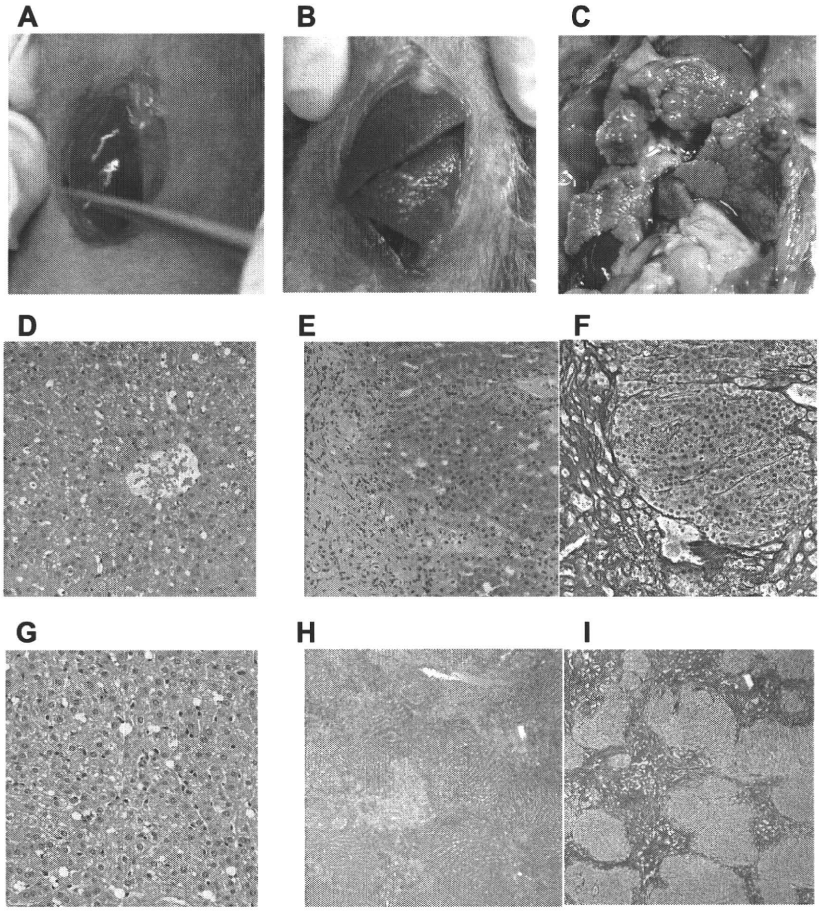

FIG. 3. Macro- and microscopic features of tupaia liver. (A) Infection-free control tupaia (Tup.15; 92 weeks). (B) RCV-infected animal displaying liver cirrhosis (Tup.8; 84 weeks postinoculation). (C) RCV-infected animal with massive surface nodules (Tup.8; 144 weeks postinoculation). (D and G) H&E staining of the uninfected Tup.15 at 92 weeks (D) and the uninfected Tup.39 at 242 weeks (G). (E, F, H, and I) H&E and silver staining of Tup.8 at 84 weeks postinoculation (E and F) or at 144 weeks postinoculation (H and I).

hepatitis had worsened with time in all HCV-infected tupaias (Fig. 2A to H and Table 2).

Fibrosis and cirrhosis were also examined. Mild fibrosis was seen in Tup.6, while severe fibrosis was seen in Tup.8. Cirrhosis was histologically investigated in all animals (Table 2). There was no significant difference between groups I and III at 94 weeks postinfection ($P = 0.194$), but at 144 weeks postinfection, a slight difference was observed ($P = 0.059$; SPSS 12.0). Macroscopic observation of the liver biopsy specimens (taken 2 years postinoculation) indicated liver cirrhosis in Tup.8 (Fig. 3B) compared with Tup.15 (uninfected control) (Fig. 3A), while silver staining of histology samples revealed fibrosis and cirrhotic nodules (Fig. 3E and F). Macroscopic observation upon sacrifice (3 years postinoculation) indicated that liver cirrhosis in Tup.8 had worsened (Fig. 3C). In contrast, age-matched infection-free negative control tupaias displayed none of these pathologies (Fig. 3A, D, and G).

Progressive lipid degeneration was noted in infected tupaias throughout the course of infection (Fig. 4). In particular, Tup.5 displayed microvesicular lipid droplets in the first biopsy specimens (at 2 years), which developed into macrovesicular droplets and foamy degeneration in biopsy specimens at 3 years (Fig. 4C and D). Liver specimens from other infected animals displayed intracellular micro- and macrovesicular lipid droplets in hepatocytes at 3 years postinoculation (Fig. 4F, H, and J). These anomalies were not present in liver specimens from infection-free control animals (Fig. 4A and B).

Transmission of viral-RNA-positive serum to naive animals reproduces acute hepatitis and viremia. To confirm virion regeneration in vivo, and to exclude the possibility of false-positive serum HCV RNA results due to amplification of the original inocula, HCV RNA-positive sera from primary inoculated tupaias were used to inoculate naive tupaias. Three different sera were tested in this passage experiment, with two naive tupaias used as recipient animals for each trial (see Materials and Methods) (Table 1, group II).

In the first reinfection experiment, serum from Tup.5 (originally infected with patient serum HCR6) was collected at 5 weeks postinoculation and used to infect two naive animals. The recipient animals showed intermittent viremia over the subsequent 3 months (Fig. 5A). In the second and third cases of reinfection, sera from Tup.8 at 10 weeks postinoculation and from Tup.4 at 8 weeks postinoculation also induced viremia in the naive inoculated animals, similar to the first reinfection experiment (Fig. 5B and C). Furthermore, the PCR titers of the recipient tupaias were significantly greater than the inoc-

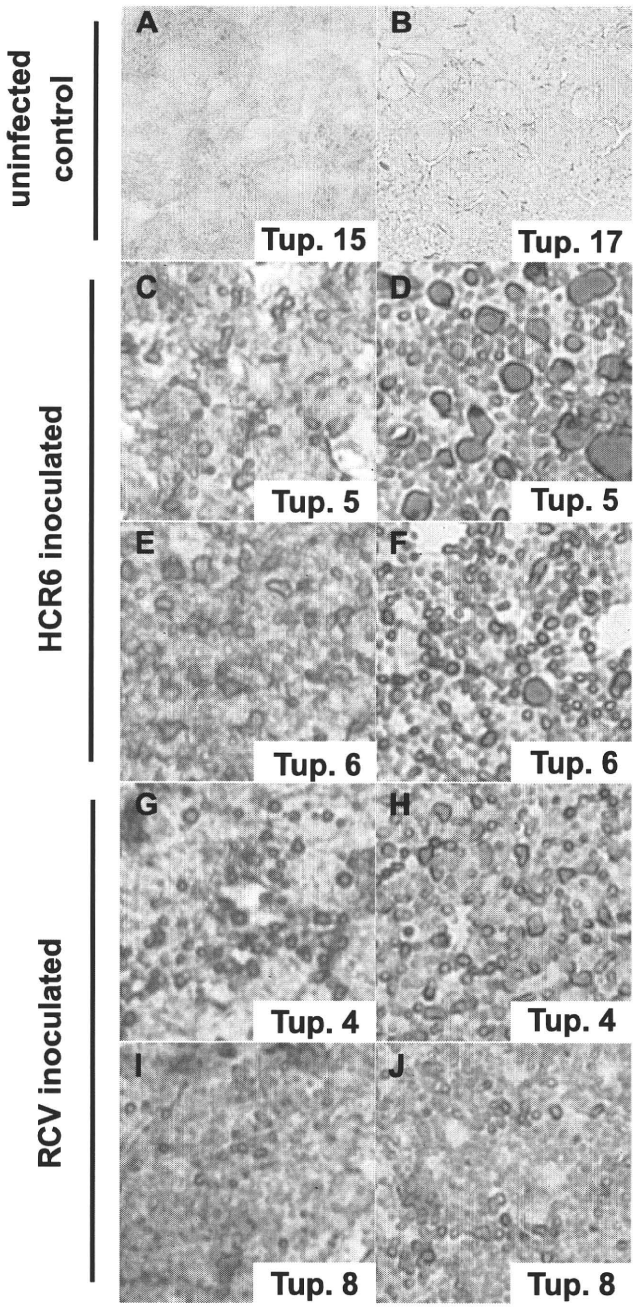

FIG. 4. Sudan IV-stained liver specimens exhibiting fatty liver degeneration. Cryosections of liver stained by Sudan IV as described in Materials and Methods show fatty liver degeneration. The left and right columns display biopsy specimens of infected animals (2 years postinoculation) and animals sacrificed at 3 years postinfection, respectively. (A and B) Uninfected controls at 2 years (Table 1 shows sample timing). (C to F) Patient serum HCR6-infected animals. (G to J) RCV-infected animals.

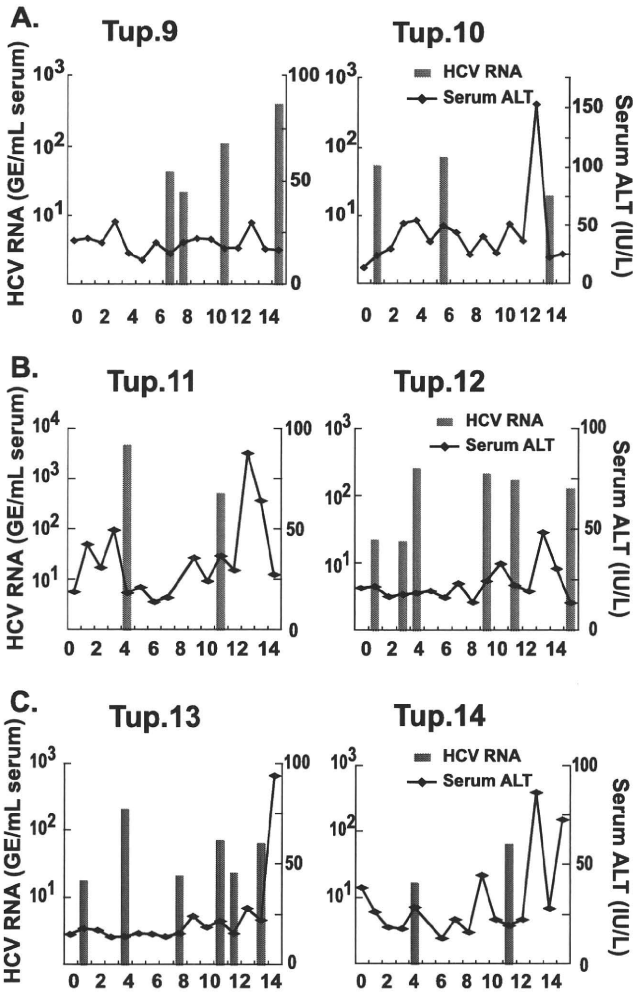

FIG. 5. Results of a reinfection experiment. (A) Quantitative RTD-PCR for HCV RNA and serum ALT levels are shown. Two naive animals were inoculated with tupaia serum (using serum taken at 5 weeks postinoculation from Tup.5, originally inoculated with patient serum HCR6) containing 100 genome equivalents (GE)/ml and were monitored for 15 weeks postinoculation (Table 1). (B) Tupaia serum (taken at 10 weeks postinoculation from Tup.8, originally inoculated with RCV) that was positive for HCV RNA was passaged into two naive animals. The animals were inoculated with tupaia serum at 100 GE/animal and monitored for 15 weeks postinoculation. (C) Tupaia serum (taken at 8 weeks postinoculation from Tup.4, originally inoculated with RCV) that was positive for HCV RNA was passaged into naive animals. The animals were inoculated with serum at 100 GE/animal and monitored for 20 weeks postinoculation.

ulation titers (10^2 genome equivalents/animal) (Table 1). For Tup.11, serum from 4 weeks postinoculation contained almost 10^4 genome equivalents/ml of HCV RNA (Fig. 5B). In addition, significant increases in serum ALT accompanied detection of serum HCV RNA. These results indicate that HCV RNA-positive sera from group I actually contained infectious virion particles. They also suggest that reconstituted HCV particles made from cDNA are infectious in tupaias.

We amplified a portion of the NS5A sequence, which is known as the interferon sensitivity determining region, by reverse transcription-PCR as described in the supplemental material. Each PCR product was subcloned and sequenced to compare the encoded amino acid sequences. For the purposes of this study, animals were inoculated with a molecular clonal virus consisting of a unique viral sequence of cDNA. The interferon sensitivity determining region sequences recovered from an animal infected with clonal inoculum (Tup.8 at 103 weeks postinoculation) were found to be heterogeneous, with

a few amino acid substitutions (K2212M for 2/10 cases, L2232P for 1/10 cases, and L2253S for 6/10 cases) (see Fig. S2E in the supplemental material). Interestingly, the codon for amino acid 2224 encodes valine, but it was found to be variant for alanine and valine in sequences from the original patient serum (HCR6). Tupaias infected with patient serum also exhibited variability at position 2224; valine occupancy was rare, as was seen in the original HCR6 population (see Fig. S2B and C in the supplemental material). On the other hand, this position was occupied solely by valine for sequences recovered from Tup.8 (see Fig. S2E in the supplemental material), indicating that genetic variations shown for Tup.8 originated from the pHCR6 cDNA sequence. Taken together, quasispecies detection of circulating virus represents further evidence demonstrating intrinsic replication of HCV in tupaias despite low levels and infrequent detection of viremia.

DISCUSSION

In the present study, we described persistent HCV infection in tupaias. Long-term follow-up was performed and revealed histological progression of HCV-related liver disorders in infected tupaias, including steatosis, fibrosis, and cirrhosis, in addition to acute and chronic hepatitis. HCV genomic RNA was detected in animal sera intermittently throughout the entire course of infection. However, HCV RNA was detected in the liver upon sacrifice (3 years postinoculation). Furthermore, HCV RNA in serum contained genomic variants that had diverged from the inoculated virus (see Fig. S1 and S2 in the supplemental material). These data strongly indicate an established persistent infection in the tupaias studied. All animals exhibited HCV viremia soon after inoculation, yet the viremia was intermittent and accompanied by relatively low RTD-PCR titers compared with equivalent human and chimpanzee infections. The discrepancy between humans and tupaias might be due to host-dependent differences in replication efficiency. Over the course of HCV infection in these tupaias, serum ALT profiles indicated repeated liver injury, probably due to host immune responses mediated by agents such as cytotoxic T lymphocytes rather than direct viral cytopathic effects.

In cases of tupaia infection, experimental inoculations rarely led to sustained viremia, which for most human cases lasts for the entire course of infection. Even the course of infection appeared transient and self-resolved. It seems likely that HCV replication is less compatible with the tupaia host environment. This possibility was substantiated by a previous report by Xu et al. (34), where tissue-cultured virions of cloned genotype 1b, referred to as HCVcc in the paper, could not cause chronic infection with sustained viremia in tupaias. Although HCVcc actually infected most of the inoculated tupaias (83%; 10/12), chronic infection was seen for only a fraction of them (20%; 2/10). In this study, we also tried to detect a humoral response to HCV core antigen. We found that tupaia sera were HCV positive for antibodies only at occasional time points, observable as intermittent steep responses (data not shown). Overall, sustained seroconversion was not seen in this study, probably because HCV propagation in vivo was so limited or well controlled by host immunity. Given that models of HCV propagation are severely limited, the most important and interesting finding of this study is the successful detection of HCV RNA in livers of infected tupaias 3 years after inoculation, indicating that HCV persists in tupaias. Although the limited propagation of HCV in tupaias is a drawback of this model at the present time, the isolation of tupaia-adapted HCV may be feasible by performing multiple infection passages. This possibility is supported by both quasispecies development and successful reinfection.

The chimpanzee is the animal species most closely related to humans, and as a model, it has contributed significantly to our understanding of HCV infection and pathogenesis. However, reproducing HCV pathogenesis in humans or chimpanzees can take as long as 10 to 20 years. The chronically infected tupaias in the present study developed complicated liver disorders in a much shorter time. Using tupaias, with their relatively short life span (3 to 5 years in the laboratory), as a model of HCV infection, we can evaluate HCV pathogenesis and correlate senescence and duration of infection.

The recent development of a primary human hepatocyte xenograft-uPA/SCID mouse model opened up opportunities to test putative antivirals against HCV replication in vivo (10, 17). In this innovative model, human hepatocytes, which are transplanted into the lobe of a mouse liver, can support HCV replication effectively. As a result, the level of circulating HCV RNA is comparable to that of a human patient. However, this mouse model is immunodeficient, and thus, it lacks the interplay between host immunity and viral infection. Therefore, it does not provide a suitable platform for characterizing immune responses to HCV infection.

HCV infection in tupaias represents an important model of HCV infection, particularly for the study of key determinants controlling virus propagation in vivo. The pathogenesis of HCV infection can be substantially different among humans, chimpanzees, and tupaias, and the mechanisms governing these differences are of great interest. Comparative studies of HCV infection in these different species will help us to understand the basic mechanisms of persistent infection.

ACKNOWLEDGMENTS

We thank Masahiro Shuda for helpful assistance and Etsuko Endo for creating the figures. We also thank the staffs of the Departments of Microbiology and Cell Biology and Mitsugu Takahashi for breeding the tupaias.

This study was supported by grants from the Ministry of Education, Culture, Sports, Science and Technology of Japan; the Program for Promotion of Fundamental Studies in Health Sciences of the Pharmaceuticals and Medical Devices Agency of Japan; and the Ministry of Health, Labor and Welfare of Japan.

REFERENCES

1. **Abe, K., T. Kurata, Y. Teramoto, J. Shiga, and T. Shikata.** 1993. Lack of susceptibility of various primates and woodchucks to hepatitis C virus. J. Med. Primatol. **22:**433–434.
2. **Aoki, Y., H. Aizaki, T. Shimoike, H. Tani, K. Ishii, I. Saito, Y. Matsuura, and T. Miyamura.** 1998. A human liver cell line exhibits efficient translation of HCV RNAs produced by a recombinant adenovirus expressing T7 RNA polymerase. Virology **250:**140–150.
3. **Chomczynski, P., and N. Sacchi.** 1987. Single-step method of RNA isolation by acid guanidinium thiocyanate-phenol-chloroform extraction. Anal. Biochem. **162:**156–159.
4. **Choo, Q. L., G. Kuo, A. J. Weiner, L. R. Overby, D. W. Bradley, and M. Houghton.** 1989. Isolation of a cDNA clone derived from a blood-borne non-A, non-B viral hepatitis genome. Science **244:**359–362.
5. **Dash, S., G. Kalkeri, H. M. McClure, R. F. Garry, S. Clejan, S. N. Thung, and K. K. Murthy.** 2001. Transmission of HCV to a chimpanzee using virus

particles produced in an RNA-transfected HepG2 cell culture. J. Med. Virol. **65**:276–281.
6. **Flugge, P., E. Fuchs, E. Gunther, and L. Walter.** 2002. MHC class I genes of the tree shrew Tupaia belangeri. Immunogenetics **53**:984–988.
7. **Goldsmith, E. I.** 1978. The convention on international trade in endangered species of wild fauna and flora. J. Med. Primatol. **7**:122–124.
8. **Hong, Z., M. Beaudet-Miller, R. E. Lanford, B. Guerra, J. Wright-Minogue, A. Skelton, B. M. Baroudy, G. R. Reyes, and J. Y. Lau.** 1999. Generation of transmissible hepatitis C virions from a molecular clone in chimpanzees. Virology **256**:36–44.
9. **Hoofnagle, J. H.** 2002. Course and outcome of hepatitis C. Hepatology **36**:S21–S29.
10. **Inoue, K., T. Umehara, U. T. Ruegg, F. Yasui, T. Watanabe, H. Yasuda, J. M. Dumont, P. Scalfaro, M. Yoshiba, and M. Kohara.** 2007. Evaluation of a cyclophilin inhibitor in hepatitis C virus-infected chimeric mice in vivo. Hepatology **45**:921–928.
11. **Ishak, K., A. Baptista, L. Bianchi, F. Callea, J. De Groote, F. Gudat, H. Denk, V. Desmet, G. Korb, R. N. MacSween, et al.** 1995. Histological grading and staging of chronic hepatitis. J. Hepatol. **22**:696–699.
12. **Ito, T., K. Yasui, J. Mukaigawa, A. Katsume, M. Kohara, and K. Mitamura.** 2001. Acquisition of susceptibility to hepatitis C virus replication in HepG2 cells by fusion with primary human hepatocytes: establishment of a quantitative assay for hepatitis C virus infectivity in a cell culture system. Hepatology **34**:566–572.
13. **Kock, J., M. Nassal, S. MacNelly, T. F. Baumert, H. E. Blum, and F. von Weizsacker.** 2001. Efficient infection of primary tupaia hepatocytes with purified human and woolly monkey hepatitis B virus. J. Virol. **75**:5084–5089.
14. **Kolykhalov, A. A., E. V. Agapov, K. J. Blight, K. Mihalik, S. M. Feinstone, and C. M. Rice.** 1997. Transmission of hepatitis C by intrahepatic inoculation with transcribed RNA. Science **277**:570–574.
15. **Major, M. E., and S. M. Feinstone.** 1997. The molecular virology of hepatitis C. Hepatology **25**:1527–1538.
16. **Marcellin, P., T. Asselah, and N. Boyer.** 2002. Fibrosis and disease progression in hepatitis C. Hepatology **36**:S47–S56.
17. **Mercer, D. F., D. E. Schiller, J. F. Elliott, D. N. Douglas, C. Hao, A. Rinfret, W. R. Addison, K. P. Fischer, T. A. Churchill, J. R. Lakey, D. L. Tyrrell, and N. M. Kneteman.** 2001. Hepatitis C virus replication in mice with chimeric human livers. Nat. Med. **7**:927–933.
18. **Nascimbeni, M., E. Mizukoshi, M. Bosmann, M. E. Major, K. Mihalik, C. M. Rice, S. M. Feinstone, and B. Rehermann.** 2003. Kinetics of CD4+ and CD8+ memory T-cell responses during hepatitis C virus rechallenge of previously recovered chimpanzees. J. Virol. **77**:4781–4793.
19. **Pawlotsky, J. M.** 2002. Use and interpretation of virological tests for hepatitis C. Hepatology **36**:S65–S73.
20. **Ren, S., and M. Nassal.** 2001. Hepatitis B virus (HBV) virion and covalently closed circular DNA formation in primary tupaia hepatocytes and human hepatoma cell lines upon HBV genome transduction with replication-defective adenovirus vectors. J. Virol. **75**:1104–1116.
21. **Seeff, L. B.** 2002. Natural history of chronic hepatitis C. Hepatology **36**:S35–S46.
22. **Shimayama, T., S. Nishikawa, and K. Taira.** 1995. Generality of the NUX rule: kinetic analysis of the results of systematic mutations in the trinucleotide at the cleavage site of hammerhead ribozymes. Biochemistry **34**:3649–3654.
23. **Shimizu, Y. K., H. Igarashi, T. Kanematu, K. Fujiwara, D. C. Wong, R. H. Purcell, and H. Yoshikura.** 1997. Sequence analysis of the hepatitis C virus genome recovered from serum, liver, and peripheral blood mononuclear cells of infected chimpanzees. J. Virol. **71**:5769–5773.
24. **Shimizu, Y. K., A. Iwamoto, M. Hijikata, R. H. Purcell, and H. Yoshikura.** 1992. Evidence for in vitro replication of hepatitis C virus genome in a human T-cell line. Proc. Natl. Acad. Sci. USA **89**:5477–5481.
25. **Suh, Y. A., P. K. Kumar, K. Taira, and S. Nishikawa.** 1993. Self-cleavage activity of the genomic HDV ribozyme in the presence of various divalent metal ions. Nucleic Acids Res. **21**:3277–3280.
26. **Takeuchi, T., A. Katsume, T. Tanaka, A. Abe, K. Inoue, K. Tsukiyama-Kohara, R. Kawaguchi, S. Tanaka, and M. Kohara.** 1999. Real-time detection system for quantification of hepatitis C virus genome. Gastroenterology **116**:636–642.
27. **Tanaka, T., N. Kato, M. J. Cho, K. Sugiyama, and K. Shimotohno.** 1996. Structure of the 3′ terminus of the hepatitis C virus genome. J. Virol. **70**:3307–3312.
28. **Thomson, M., M. Nascimbeni, M. B. Havert, M. Major, S. Gonzales, H. Alter, S. M. Feinstone, K. K. Murthy, B. Rehermann, and T. J. Liang.** 2003. The clearance of hepatitis C virus infection in chimpanzees may not necessarily correlate with the appearance of acquired immunity. J. Virol. **77**:862–870.
29. **Tsukiyama-Kohara, K., N. Iizuka, M. Kohara, and A. Nomoto.** 1992. Internal ribosome entry site within hepatitis C virus RNA. J. Virol. **66**:1476–1483.
30. **Tsukiyama-Kohara, K., S. Tone, I. Maruyama, K. Inoue, A. Katsume, H. Nuriya, H. Ohmori, J. Ohkawa, K. Taira, Y. Hoshikawa, F. Shibasaki, M. Reth, Y. Minatogawa, and M. Kohara.** 2004. Activation of the CKI-CDK-Rb-E2F pathway in full genome hepatitis C virus-expressing cells. J. Biol. Chem. **279**:14531–14541.
31. **Walter, E., R. Keist, B. Niederost, I. Pult, and H. E. Blum.** 1996. Hepatitis B virus infection of tupaia hepatocytes in vitro and in vivo. Hepatology **24**:1–5.
32. **Wasley, A., and M. J. Alter.** 2000. Epidemiology of hepatitis C: geographic differences and temporal trends. Semin. Liver Dis. **20**:1–16.
33. **Xie, Z. C., J. I. Riezu-Boj, J. J. Lasarte, J. Guillen, J. H. Su, M. P. Civeira, and J. Prieto.** 1998. Transmission of hepatitis C virus infection to tree shrews. Virology **244**:513–520.
34. **Xu, X., H. Chen, X. Cao, and K. Ben.** 2007. Efficient infection of tree shrew (Tupaia belangeri) with hepatitis C virus grown in cell culture or from patient plasma. J. Gen. Virol. **88**:2504–2512.
35. **Yanagi, M., R. H. Purcell, S. U. Emerson, and J. Bukh.** 1997. Transcripts from a single full-length cDNA clone of hepatitis C virus are infectious when directly transfected into the liver of a chimpanzee. Proc. Natl. Acad. Sci. USA **94**:8738–8743.
36. **Yanagi, M., M. St Claire, M. Shapiro, S. U. Emerson, R. H. Purcell, and J. Bukh.** 1998. Transcripts of a chimeric cDNA clone of hepatitis C virus genotype 1b are infectious in vivo. Virology **244**:161–172.
37. **Zhao, X., Z. Y. Tang, B. Klumpp, G. Wolff-Vorbeck, H. Barth, S. Levy, F. von Weizsacker, H. E. Blum, and T. F. Baumert.** 2002. Primary hepatocytes of Tupaia belangeri as a potential model for hepatitis C virus infection. J. Clin. Invest. **109**:221–232.

Journal of Medical Virology 82:1545–1553 (2010)

Natural Killer Cells Target HCV Core Proteins During the Innate Immune Response in HCV Transgenic Mice

Kenichi Satoh,[1,2] Hiroki Takahashi,[2] Chiho Matsuda,[1] Toshiyuki Tanaka,[3] Masayuki Miyasaka,[4] Mikio Zeniya,[2] and Michinori Kohara[1]*

[1]*Department of Microbiology and Cell Biology, The Tokyo Metropolitan Institute of Medical Science, Bunkyo-ku, Tokyo, Japan*
[2]*Division of Gastroenterology and Hepatology, Department of Internal Medicine, The Jikei University School of Medicine, Minato-ku, Tokyo, Japan*
[3]*Laboratory of Immunobiology, Department of Pharmacy, School of Pharmacy, Hyogo University of Health Sciences, Chuo-ku, Kobe, Japan*
[4]*Laboratory of Immunodynamics, Department of Microbiology and Immunology, Osaka University Graduate School of Medicine, Suita, Osaka, Japan*

The mechanism of the innate immune response to hepatitis C virus (HCV) has not been fully elucidated, largely due to the lack of an appropriate model. We used HCV transgenic (Tg) mice, which express core, E1, E2, and NS2 proteins regulated by the Cre/*loxP* switching expression system, to examine the innate immune response to HCV structural proteins. Twelve hours after HCV transgene expression, HCV core protein levels in Tg mouse livers were 15–47 pg/mg. In contrast, in Tg mice with a depletion of natural killer (NK) cells, we observed much higher levels of HCV core proteins (1,597 pg/ml). Cre-mediated genomic DNA recombination efficiency in the HCV-Tg mice was strongly observed in NK cell-depleted mice between 0.5 and 1 day as compared to non-treated mice. These data indicated that NK cells participate in the elimination of core-expressing hepatocytes in the innate immune responses during the acute phase of HCV infection. ***J. Med. Virol. 82:1545–1553, 2010.***

KEY WORDS: HCV; Cre/loxP switching Tg; innate immunity; natural killer cell; core protein

INTRODUCTION

Although a variety of studies have demonstrated that infection with hepatitis C virus (HCV) elicits an innate immune response in human hosts, the mechanisms behind this response are not well understood. Details on the first step of the immune process might assist in the development of treatments for chronic hepatitis, cirrhosis, and hepatocellular carcinoma. One of the factors limiting such HCV immune research is the general lack of animal models: Humans are the only natural HCV host, and to date, chimpanzees are the only animals that have been infected with HCV.

Clinically, approximately 50% of symptomatic patients eliminate the virus, whereas in an asymptomatic course, more than 80% of acute HCV infections develop into chronic infection [Gerlach et al., 2003], indicating that the infected host's immune reaction may influence the course of the disease. In the chimpanzee model, HCV significantly induces type I interferon (IFN) [Bigger et al., 2001; Su et al., 2002]. However, this response occurs irrespective of the outcome of infection [Disson et al., 2004; Machida et al., 2001; Su et al., 2002; Thimme et al., 2002], and NS3-4A can inhibit RIG-1-mediated signaling, which is required to be activated for IFN production [Vilasco et al., 2006].

Natural killer (NK) cells constitute the first line of host defense against invading pathogens and are usually activated in the early phase of viral infection.

Abbreviations used: HCV, hepatitis C virus; NK cell, natural killer cell; IFN, interferon; Tg, transgenic; ALT, alanine aminotransferase; IRF, interferon regulatory factor.

Grant sponsor: Ministry of Education, Culture, Sports, Science and Technology of Japan; Grant sponsor: Program for Promotion of Fundamental Studies in Health Sciences of the National Institute of Biomedical Innovation of Japan; Grant sponsor: Ministry of Health, Labor and Welfare of Japan.

*Correspondence to: Michinori Kohara, PhD, Department of Microbiology and Cell Biology, The Tokyo Metropolitan Institute of Medical Science, 2-1-6 Kamikitazawa, Setagaya-ku, Tokyo 156-8506, Japan. E-mail: kohara-mc@igakuken.or.jp

Accepted 28 April 2010
DOI 10.1002/jmv.21859
Published online in Wiley InterScience (www.interscience.wiley.com)

The liver is particularly enriched with NK cells, which are activated by hepatotropic viruses such as HCV. There have been some reports of the association between NK cells and HCV [Ebihara et al., 2008; Knapp et al., 2009; Vidal-Castineira et al., 2010]. For instance, NK cell numbers were consistently lower in individuals with persistent HCV infections [Golden-Mason et al., 2008]. Additionally, the function of NK cells can be inhibited by HCV proteins such as envelope protein E2, which impairs the effector function of NK cells by interacting with CD81 on their surface [Crotta et al., 2002; Tseng and Klimpel, 2002].

Most of these studies on the association between NK cells and HCV have been performed during the chronic phase of HCV infection. To our knowledge, there has been no research on the innate immune response during the acute phase of HCV infection, because of the difficulty in analyzing early immune reactions and the lack of appropriate animal models. Here, we have overcome this difficulty by using the Cre/*loxP* system to create a mouse model with conditional HCV transgene expression. This allowed us to analyze HCV-specific innate immunity.

MATERIALS AND METHODS

HCV Transgenic Mice

HCV-Tg mice CN2-8 and CN2-29 (BALB/c, 9- to 12-week old) were used in the experiments. These two Tg mice lineages possess HCV genotype 1b, which is regulated by the Cre/*loxP* conditional switching system [Wakita et al., 1998]. NK cell- and $CD8^+$ T-cell-deficient HCV-Tg mice were also established by mating HCV-Tg mice with syngenic IRF-1-deficient mice, in which a strong reduction in NK cells [Duncan et al., 1996; Ohteki et al., 1998] and $CD8^+$ T cells [Matsuyama et al., 1993] has been reported.

All mice were cared for according to the guidelines of the NIH Guide for the Care and Use of Laboratory Animals.

Structure of CALCN2, the Cre-Mediated Activation Transgene Unit

R6CN2 HCV cDNA (nucleotides: 294–3,435, aa: 1–1,013) contains the core, E1, E2, and NS2 regions. This construct does not lead to HCV mRNA transcription before recombination. It was cloned downstream of the CAG promoter, neomycin-resistant gene (*neo*), and poly(A) signal; the latter two of these were flanked by *loxP* sequences. The CAG promoter comprises, in order, the cytomegalovirus enhancer, actin promoter, and the globin poly(A) signal. CALNCN2, the Cre-mediated activation transgene unit, consists of the CAG promoter, a *loxP* sequence, the *neo*-resistance gene, the SV40 poly(A) signal, a second *loxP* sequence, R6CN2 HCV cDNA, and the globin poly(A) signal, in that order.

Upon recognition of the *loxP* site, Cre recombinase deletes the neo gene and the SV40 poly(A) signal, along with one of the *loxP* sequences. It then ligates the CAG promoter to the HCV cDNA and the globin poly(A) signal. This genomic structure alteration enables the production of HCV mRNA [Wakita et al., 1998].

Hydrodynamics-Based Transfection of Naked Plasmid DNA

Cre recombinase cDNA (pCAN-Cre/pBR325 plasmid) was cloned downstream of the CMV promoter. Plasmid DNA was prepared using the triton-cesium chloride method. Plasmid DNA (20 μg) was diluted with 2.0 ml of PBS(−) mixed with atelocollagen (KOKENCELLGEN I-AC; Koken, Tokyo, Japan) [Ochiya et al., 2001; Minakuchi et al., 2004] to a final concentration of 0.01%. This was then injected via a tail vein, after which it entered circulation within 6–8 sec [Liu et al., 1999].

Depletion of NK Cells

Transgenic mice were treated intraperitoneally with 1 mg of anti-IL2 receptor-β monoclonal antibody (TM-βI, rat IgG2b) [Tanaka et al., 1993] in 500 μl of PBS(−) once, 2 days before Cre/loxP switching.

Quantification of HCV Core Proteins in Mouse Livers

Hepatocyte HCV core protein concentrations were quantified with a fluorescent enzyme immunoassay (FEIA) by using HCV core monoclonal antibodies from a commercial kit, as previously described [Kashiwakuma et al., 1996].

Immunoblot Analysis

Liver tissues (100–150 μg) were lysed with 300 μl of RIPA buffer (1% SDS, 0.5% Nonidet P40, 0.5 mmol/L EDTA,150 mmol/L NaCl, and 1 mmol/L DTT and 10 mmol/L Tris, pH 7.4). After the supernatant protein concentration was determined, 30 μg of total protein was electrophoresed on SDS–PAGE (15% polyacrylamide) and transferred to a polyvinylidene difluoride (PVDF) membrane (Immobilon-P, Millipore, Bedford, MA). The membrane was incubated with biotinylated 515S (an anti-HCV core monoclonal antibody), 384 (an anti-HCV E1 monoclonal antibody), or 541 (an anti-HCV E2 monoclonal antibody) [Tsukiyama-Kohara et al., 2004], followed by horseradish peroxidase-conjugated streptavidin. Proteins were visualized using the ECL system (Amersham Biosciences, Cleveland, OH).

Southern Blotting

Genomic DNA (4 μg) was extracted from mouse liver tissue by using the phenol–chloroform method. It was digested with *Xba*I and then resolved by electrophoresis on a 0.8% agarose gel. Bands were transferred to a Hybond-N membrane (Amersham Biosciences) by using the Vacugene 2016 (LKB Biotechnology, Bromma, Sweden). The blots were then probed with a ^{32}P-dCTP-

labeled CALNCN2 (nucleotides: 483–1,389) probe. The probe was generated using a Random Primer DNA Labeling Kit, Ver 2.0 (Takara, Shiga, Japan).

Northern Blotting

Total RNA (30 μg) was extracted from mouse liver tissue by using the AGPC method. Bands were transferred to a Hybond-N membrane (Amersham Biosciences). The blots were then probed with the same probe used for Southern blotting.

Expression Plasmids of HCV Structural Proteins

We generated expression plasmids of HCV-core (aa: 1–192; pEF-core), HCV-E1 (aa: 168–383; pEF-E1), and HCV-E2 (aa: 367–830; pEF-E2) [Takaku et al., 2003] under the control of the EF2-α promoter, and HCV-CN2 (aa: 1–1,013; pCAL CN2) [Tsukiyama-Kohara et al., 2004] and β-lactamase (pCAL-LacZ), under the control of the CAG promoter.

Cytokine Assay

Secretion of serum IFN-γ [Carroll et al., 1997], IL-12, and TNF-α was measured using enzyme-linked immunosorbent assay kits (BioSource, Camarillo, CA), according to the manufacturer's protocols.

Assay of Alanine Aminotransferase (ALT) Levels

Serum ALT concentrations were determined with a Transferase Nissui kit (Nissui Pharmaceutical Co., Tokyo, Japan) and then standardized and expressed as IU/L.

RESULTS

HCV Core Protein and ALT Levels During the Early Phase of HCV Transgenic Mouse

In CN2-8 Tg mice, HCV core protein expression levels were as follows: day 0.5: 15 ± 16 pg/mg; day 1: 175 ± 96 pg/mg; day 2: 207 ± 77 pg/mg; day 3: 33 ± 41 pg/mg; day 4: 431 ± 256 pg/mg; day 14: 4 ± 1 pg/mg (Fig. 1A). In the CN2-29 Tg mice, HCV core protein expression levels were as follows: day 0.5: 47 ± 13 pg/mg; day 1: 495 ± 165 pg/mg; day 2: 1189 ± 210 pg/mg; day 3: 26 ± 39 pg/mg; day 4: 59 ± 49 pg/mg; day 14: 2 ± 2 pg/mg (Fig. 1B). ALT levels were 489 ± 150 IU/L in the CN2-8 Tg mice and 2,282 ± 358 IU/L in the CN2-29 Tg mice at day 0.5, after which the levels quickly decreased. In both mice lineages, HCV core protein expression levels were low from day 8. In contrast, HCV core protein was not detected and the ALT levels were low (357 ± 150 IU/L) at day 0.5 in the CN2-29 Tg mice injected with the negative control vector (pBR325) (Fig. 1C).

In the immunoblot analysis, the HCV core (21 kDa) protein was detectable from days 0.5 to 3 (Fig. 1D). To investigate why the core protein was eliminated after day 3, we performed Southern and Northern blot analyses using liver tissue extracts. Transgene recombination occurred in the Tg mouse livers (Fig. 1E). CALNCN2 mRNA expression levels were similar throughout the study period (Fig. 1F). Although HCV mRNA was consistently observed, the HCV core protein was eliminated by day 4 (Fig. 1D), suggesting that some immune factors were active against HCV core protein from day 3 onward.

Histopathology of the HCV Protein Expressed During the Early Phase of HCV Transgenic Mouse

Histopathology of the CN2-29 Tg mice (Fig. 2B–E) revealed inflammation and elevation of ALT levels in livers with HCV structural protein expression compared to that in livers without HCV structural protein expression (Fig. 2F–I). The presence of HCV structural proteins was associated with the following: hepatocyte necrosis and mononuclear cell infiltration in both the liver lobules and in the periportal area, on day 0.5 (Fig. 2B); mononuclear cell infiltration, on days 1 (Fig. 2C) and 3 (Fig. 2E); and Kupffer-like infiltrated cells, on day 2 Fig. 2D). No changes in inflammation were found in the control vector-injected mice (Fig. 2F–I).

NK Cell Activity Against Cells Expressing HCV Proteins

HCV core protein expression levels were higher in the CN2-8 IRF-1 knockout mice than in wild-type Tg mice (309 ± 76 pg/mg vs. 15 ± 16 pg/mg), while ALT levels were lower (194 ± 53 I/U vs. 489 ± 142 IU/L; Fig. 1A).

HCV core protein expression levels were higher in NK cell-depleted mice with anti-IL2 receptor-β antibodies than in non-treated CN2-29 Tg mice (1,597 ± 153 pg/mg vs. 47 ± 13 pg/mg), while ALT levels were lower (608 ± 258 IU/L vs. 2,282 ± 458 IU/L) on day 0.5 (Figs. 1B and 3). However, core protein levels were drastically reduced in the treated mice on day 2. Transgene recombination was strongly observed between days 0.5 and 1 (Fig. 3C), indicating that activated NK cells were responsible for eradicating the HCV proteins.

In BALB/c mice whose livers had been hydrodynamically transfected with the pCAL-CN2 plasmid, HCV core protein expression level was 123 ± 45 pg/mg and the ALT level was 3,256 ± 703 IU/L on day 0.5. By day 1, both the HCV core protein expression level (54 ± 65 pg/mg) and the ALT level (841 ± 174 IU/L) had decreased; they were also relatively low on day 2 (Fig. 4A).

Both the HCV core protein expression level (2,900 ± 400 pg/mg on days 0.5 and 10,700 ± 3,100 pg/mg on day 1) and the ALT level (295 ± 197 IU/L on day 0.5 and 91 ± 51 IU/L on day 1) were lower in IRF-1 knockout BALB/c mice than in wild-type BALB/c mice (Fig. 4A,B). In contrast, in wild-type BALB/c mice hydrodynamically transfected with the pCAL-LacZ plasmid, the β-galactosidase level did not dramatically change over the study period (7.9 ± 2.0 on day 0.5; 3.9 ± 2.1 on day 14). The ALT level (450 ± 90 IU/L) was lower in plasmid-transfected mice than in wild-type mice (Fig. 4A,C), but

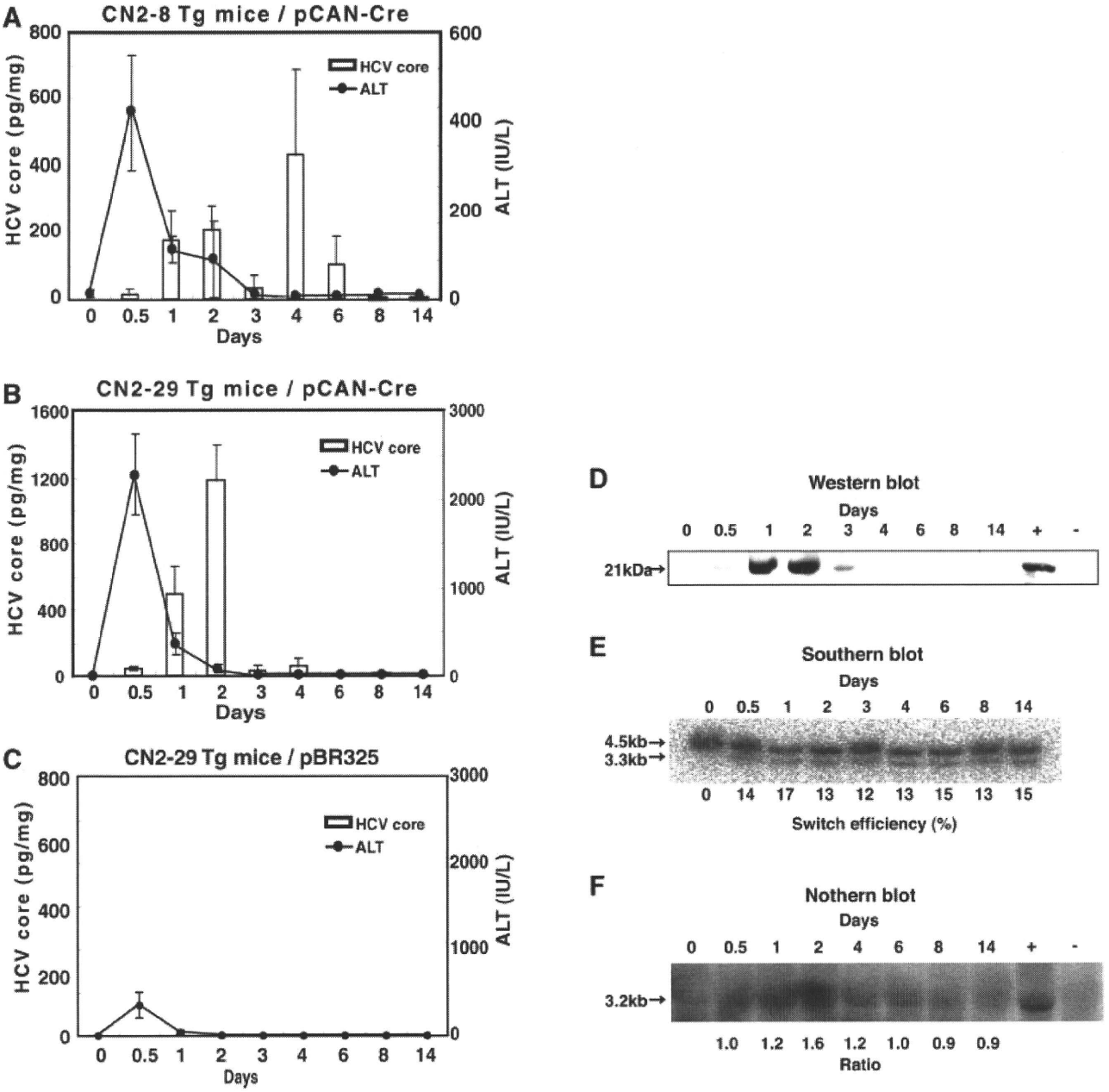

Fig. 1. Quantification of HCV core protein production and ALT levels in transgenic mice hydrodynamically transfected with the pCAN-Cre plasmid. Values for core protein and serum ALT levels represents the mean and SD from three experiments. **A**: CN2-8 transgenic mice. Analysis of quantity of core protein and serum ALT levels in the hepatocytes. Hepatitis was first detectable via elevated serum ALT activity on day 0.5, after which ALT activity rapidly rose, only to return to the baseline level after day 3. Hepatocyte core protein levels peaked twice, on day 2 (207 ± 77 pg/mg) and day 4 (431 ± 256 pg/mg). **B**: CN2-29 transgenic mice. Hepatitis was first detectable as elevated serum ALT activity on day 0.5. Serum ALT activity peaked at 2,282 ± 358 IU/L and then declined gradually from day 1 (366 ± 123 IU/L). It returned to the baseline level after day 2. Hepatocyte core protein levels were first detectable on day 0.5 (47 ± 13 pg/mg), peaked on day 2 (1,189 ± 210 pg/mg), and returned to the baseline level after day 3. **C**: Serum ALT levels in negative control plasmids (pBR325, 20 μg) injected into CN2-29 transgenic mice. The serum ALT level of the control plasmids was lower than in CN2-29 transgenic mice and was only detectable on day 0.5, after which it returned to the baseline level. Core protein levels were not detectable. **D**: Immuno-blot from the liver of a CN2-29 transgenic mouse liver hydrodynamically transfected with the pCAN-Cre plasmid. HCV core protein in the liver extract was barely detectable 12 h after switching in the CN2-29 Tg mouse, was strongly detected on days 1 and 2, and was eliminated after day 3. The density of the HCV core protein band reflected the HCV protein expression levels shown in Fig. 1B. **E**: Switching efficiency of Cre-mediated genomic DNA recombination in the liver of a CN2-29 transgenic mouse hydrodynamically transfected with the pCAN-Cre plasmid. HCV transgene recombination in the somatic tissues of pCANCre-injected mice. Southern blot analysis of tissues from CN2-29 mice. Transgene recombination was consistently observed between days 0.5 and 14. kb, kilobase pairs. **F**: Cre-mediated genomic DNA recombination and mRNA in the CN2-29 transgenic mouse liver hydrodynamically transfected with the pCAN-Cre plasmid. The expression level of CALNCN2 mRNA by Northern blot analysis.

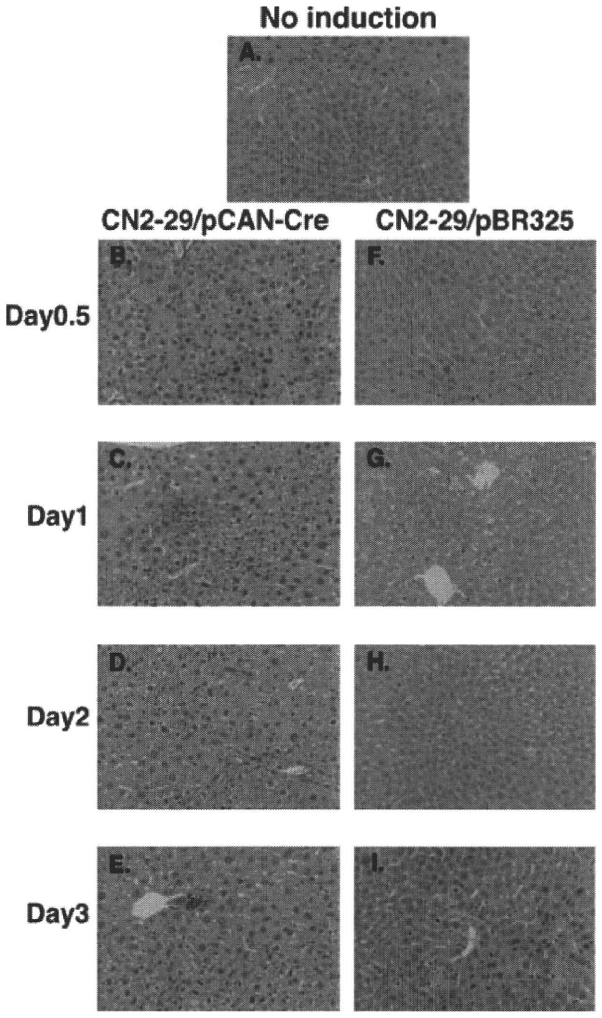

Fig. 2. Hematoxylin and eosin staining of liver sections from CN2-29 Tg mice. The presence of HCV structural proteins was associated with the following: (**B**) hepatocyte necrosis and mononuclear cell infiltration in the liver lobules and periportal area on day 0.5; (**C,E**) mononuclear cell infiltration on days 1 and 3; (**D**) Kupffer-like cell infiltration on day 2. **F–I**: No inflammation changes were seen in the liver following pBR325 plasmid injection.

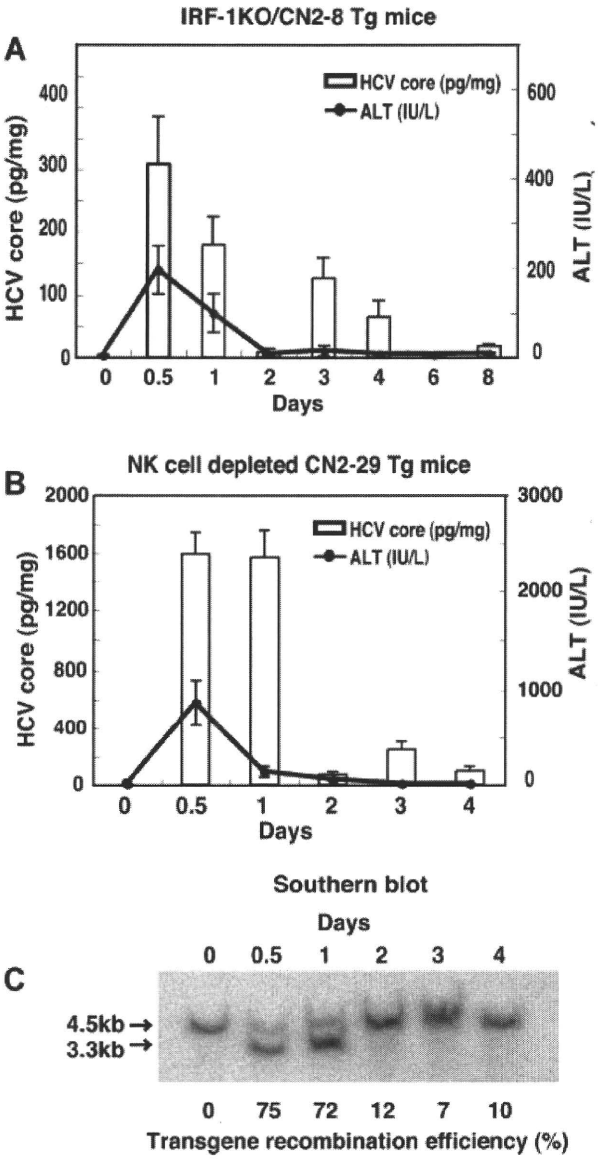

Fig. 3. Quantification of HCV core protein production and serum ALT levels in IRF-1 knockout CN2-8 transgenic mice and NK cell-depleted CN2-29 transgenic mice hydrodynamically transfected with the pCAN-Cre plasmid. **A**: HCV core protein and serum ALT levels in IRF-1 knockout CN2-8 Tg mice. The core protein level in the hepatocytes rapidly increased on day 0.5 (309 ± 76 pg/mg). The serum ALT level (194 ± 53 IU/L) was lower than in wild-type mice (490 ± 150 IU/L) on day 0.5 (Fig. 1A). **B**: HCV core protein and serum ALT levels in NK cell-depleted CN2-29 Tg mice. The core protein level in the liver rapidly increased on day 0.5 ($1,597 \pm 153$ pg/mg). The serum ALT level (489 ± 142 IU/L) was lower than in wild-type mice ($2,282 \pm 358$ IU/L) on day 0.5 (Fig. 1B). **C**: Cre-mediated genomic DNA recombination efficiency throughout the study period.

the β-galactosidase level (7.4 ± 2.5 on day 0.5 and 5.4 ± 2.3 on day 1) was comparable. Finally, the ALT level was 325 ± 178 IU/L on day 0.5 (Fig. 4D).

When the pCAN-Cre/pBR325 plasmid was injected into wild-type BALB/c mice, the results were similar to those seen in the absence of the vector (data not shown), suggesting that the pCAN-Cre plasmid injection had no effect.

Cumulatively, these findings suggest that HCV protein-expressing cells were eliminated by NK cells during the acute early phase of innate immunity.

IFN-γ Secretion Induced HCV Core Protein in the Acute Early Phase of Innate Immunity

We analyzed cytokine (IFN-γ, IL-12, and TNF-α levels from days 0 to 14 after the hydrodynamic transfection of pCAN-Cre plasmids into CN2-29 Tg mice. Serum IL-12 and TNF-α were not detected on any day during the study period (data not shown). Serum IFN-γ was detected on day 0.5 in pCAN-Cre-transfected mice, but not in control vector-injected mice (Fig. 5A).

IFN-γ was strongly secreted on day 0.5 in response to transfection with pEF-core expression plasmids (Fig. 5B), but was only slightly induced by the HCV E1 and E2 (not detected) proteins (Fig. 5B). In contrast,

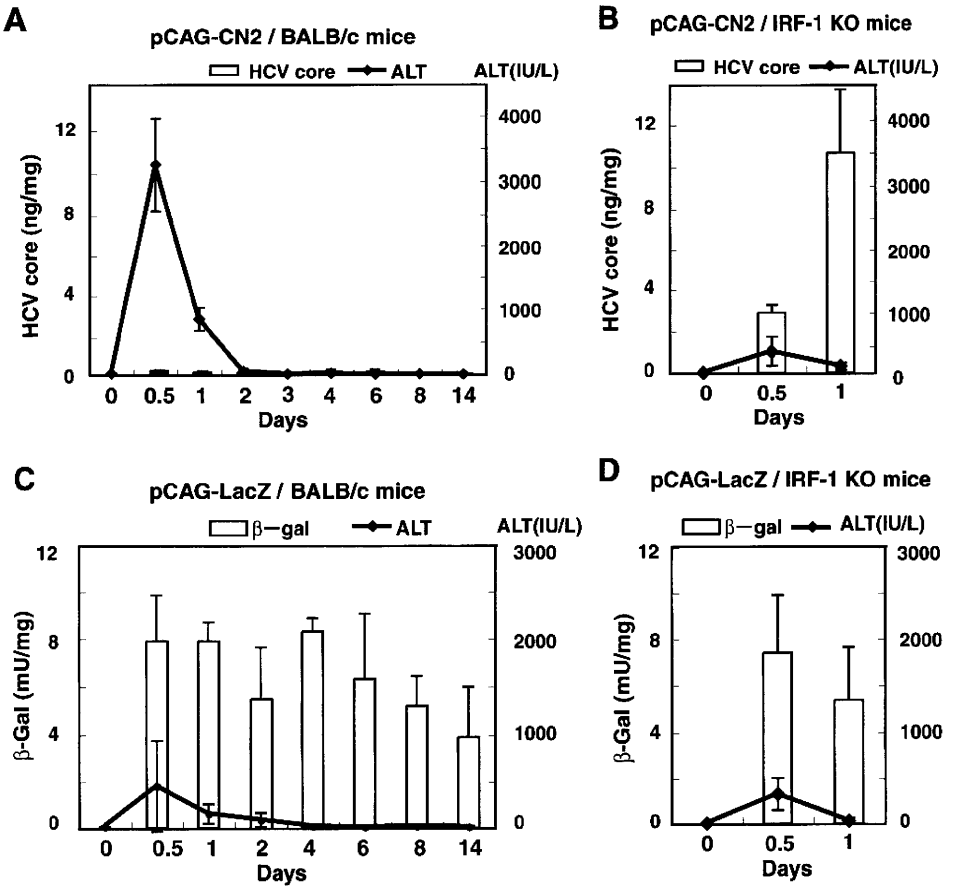

Fig. 4. Quantification of HCV core protein production and serum ALT levels in wild-type BALB/c mice and IRF-1 knockout BALB/c mice hydrodynamically transfected with expression plasmids. **A**: Results for wild-type BALB/c mice injected with pCAG-CN2 (Fse). HCV core protein in the liver was barely detectable at day 0.5 (0.123 ± 0.045 ng/mg) and declined gradually thereafter. The serum ALT level peaked on day 0.5 (3,256 ± 703 IU/L) and declined gradually thereafter. **B**: Results for IRF-1 knock out BALB/c mice injected with pCAG-CN2 (Fse). HCV core protein levels in the hepatocytes was most strongly detected on days 0.5 (2.9 ± 0.4 ng/mg) and 1 (10.7 ± 3.1 ng/mg). Serum ALT was suppressed on day 0.5 (295 ± 197 IU/L). **C**: Results for BALB/c mice injected with pCAG-LacZ. Liver β-gal levels were first detectable on day 0.5 (7.9 ± 2.0 mU/mg) and were consistently detectable until day 14 (3.9 ± 2.1 mU/mg). The serum ALT level (450 ± 490 IU/L) was lower than that shown in Figure 2A (3,256 ± 703 IU/L) at day 0.5, and returned to the baseline level after day 2. **D**: Results from IRF-1 knockout BALB/c mice injected with pCAG-LacZ. Liver β-gal levels were detected on days 0.5 (7.4 ± 2.5 mU) and 1 (5.4 ± 2.3 mU). The serum ALT level was (352 ± 178 IU/L) on day 0.5.

serum IFN-γ was not detected after transfection with pEF-core expression plasmids in CN2-8 IRF-1 (Fig. 5C). Serum IFN-γ secretion was suppressed in NK cell-depleted CN2-29 Tg mice and was not stimulated by pCAL-LacZ plasmid injection (Fig. 5D,E).

DISCUSSION

Immune responses to HCV during the acute phase of infection might play a crucial role in determining whether HCV is eliminated or is able to persist in the body. However, acute HCV infection is rarely symptomatic, making it tremendously difficult to analyze in vivo. In the present study, we generated an acute HCV model for the first time by using Tg mice with conditional expression regulated by the Cre/*loxP* system. Because there were no viral vector effects, we were able to observe HCV-specific innate immunity by using hydrodynamic transfection techniques.

NK cells constitute the first line of host defense against invading pathogens. Activated NK cells play an essential role in recruiting virus-specific T cells and inducing antiviral immunity in the liver [French et al., 2003]. They also eliminate virus-infected hepatocytes directly by cytolytic mechanisms and indirectly by secreting cytokines, which induce an antiviral state in host cells. In vitro studies revealed that NK cells are activated by cytokines during acute HCV infection [Yoon et al., 2008] and play an important antiviral role by eliminating the virus, both by killing it directly and by producing cytokines such as IFN-γ [Golden-Mason and Rosen, 2006].

In the present study, hepatocyte necrosis and intrahepatic mononuclear cell infiltration were observed on days 0.5 and 1 in wild-type mice. These were associated with elevated levels of serum ALT and IFN-γ and with reduced levels of HCV core protein expression. In contrast, NK cell depletion by IRF-1 knockout or treatment with anti-IL-2 receptor-β antibody was

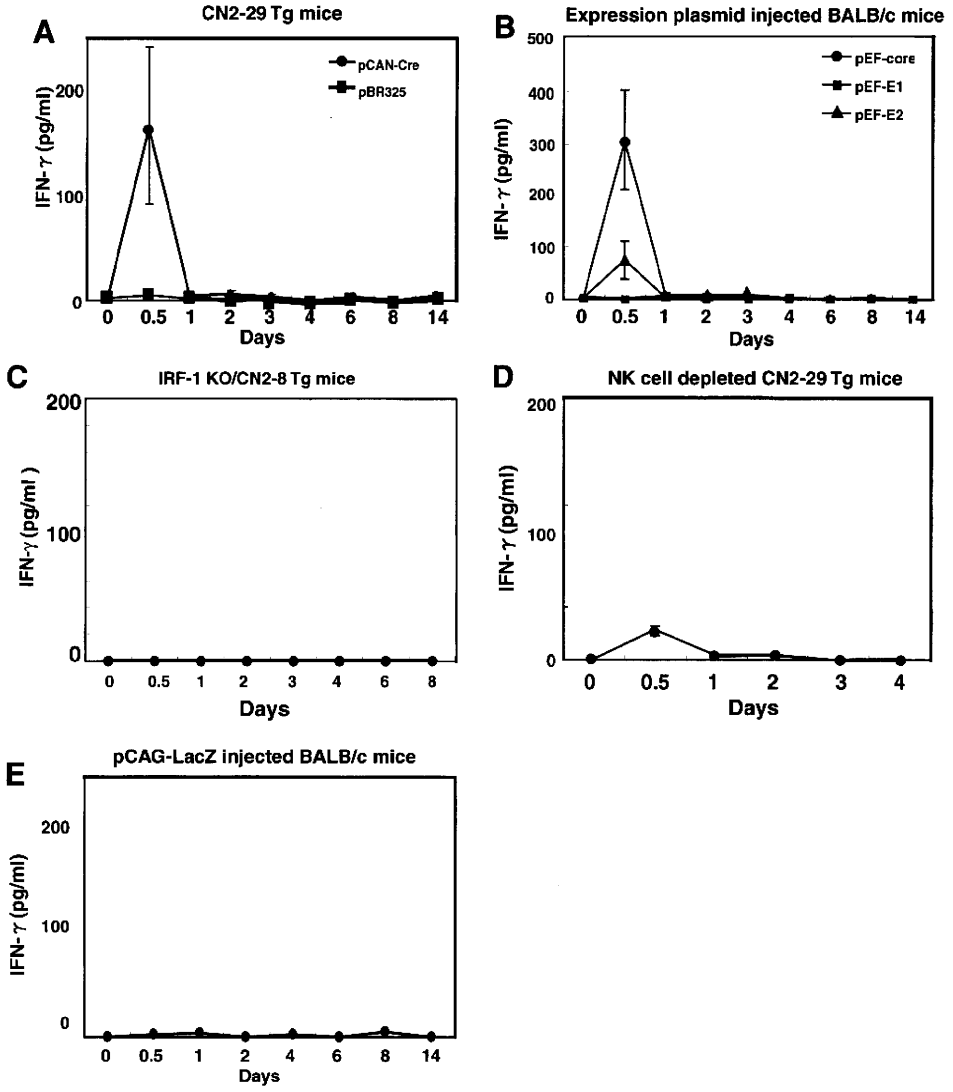

Fig. 5. Serum IFN-γ levels. **A**: Serum IFN-γ levels in CN2-29 Tg mice injected with the pCAN-Cre plasmid. Serum IFN-γ (168 ± 62 pg/ml) was detectable on day 0.5 in the pCAN-Cre plasmid-injected CN2-29 Tg mice (circle), but was not detectable in the pBR325 plasmid-injected CN2-29 Tg mice (square). **B**: Serum IFN-γ levels in mice injected with pEF-core (circle), -E1 (square), and -E2 (triangle) plasmids. **C**: Serum IFN-γ levels in IRF-1 knockout CN2-8 Tg mice injected with the pCAN-Cre plasmid. **D**: Serum IFN-γ levels in NK cell-depleted CN2-29 Tg mice injected with the pCAN-Cre plasmid. **E**: Serum IFN-γ levels in BALB/c mice injected with the pCAL-LacZ plasmid.

accompanied by increases in HCV core protein expression and decreased levels of ALT and IFN-γ on days 0.5 and 1. These results were confirmed by our histological observations. Cumulatively, these data suggest that the activity of NK cells might be directly cytolytic; specifically, they appear to play a significant role in IFN-γ secretion and elimination of virus-infected hepatocytes—especially core protein-presented hepatocytes—during the early phase of infection (days 0–1). Since the number of CD8+ cytotoxic T cells is greatly reduced in CN2-8 IRF-1 knockout mice, T cells usually participate in innate immunity, rather than acquired immunity. It has previously been reported that NK cells are required to recruit virus-specific T cells in response to HCV infection [Ahmad and Alvarez, 2004; Irshad et al., 2008]. These reports, together with our current work, indicate that NK cells play a very important antiviral role during acute HCV infection.

According to the results of the Southern and Northern blot analyses, non-cytolytic HCV core protein elimination takes place from days 3 to 14. However, this does not appear to be associated with IFN-γ or CD8+ cytotoxic T cells. Thus, during this period, another immune factor might be involved in eliminating HCV core protein in the hepatocytes without elevating ALT activity.

It is interesting that HCV core protein, but not E1 or E2 protein, induced the elevation of IFN-γ. Since HCV core protein is reported to activate NF-kB, thereby inducing the cellular inflammatory response [Dolganiuc et al., 2004], there is a possibility that HCV core protein

itself participates in the elevation of IFN-γ. IFN-γ is known to be expressed in the liver when infections spontaneously clear [Major et al., 2002; Thimme et al., 2002] and to be involved in the non-cytolytic control of HCV-infected hepatocytes [Thimme et al., 2001]. Additionally, IFN-γ inhibits the replication of subgenomic HCV replicons [Lohmann et al., 1999; Blight et al., 2000] in tissue culture cells [Frese et al., 2002; Lanford et al., 2003]. Since NK cells produce a large amount of IFN-γ when they are activated in response to inflammation, such as that caused by acute viral infection, both NK cells and IFN-γ may contribute to the innate immune response during acute HCV infection.

In conclusion, this Tg mouse model permits analysis of the HCV-specific immune response while avoiding adenovirus which has been applied for the study of HCV immunity. By using this model, we could determine some of the potential roles of NK cells in response to the presence of HCV structural protein during the early naïve phase of HCV infection. These findings confirm that NK cell activity is crucial in eliminating HCV-infected hepatocytes. This suggests that a potential new therapeutic approach is activation of NK cells in order to restore the innate immune defenses that control HCV replication.

ACKNOWLEDGMENTS

The authors wish to express their gratitude to Izumu Saito for his kind gift of the pCAN-Cre plasmid. We thank Dr. Masahiro Shuda for helpful comments during the preparation of this manuscript. We also thank Mitsugu Takahashi for breeding the transgenic mice.

REFERENCES

Ahmad A, Alvarez F. 2004. Role of NK and NKT cells in the immunopathogenesis of HCV-induced hepatitis. J Leukoc Biol 76:743–759.

Bigger CB, Brasky KM, Lanford RE. 2001. DNA microarray analysis of chimpanzee liver during acute resolving hepatitis C virus infection. J Virol 75:7059–7066.

Blight KJ, Kolykhalov AA, Rice CM. 2000. Efficient initiation of HCV RNA replication in cell culture. Science 290:1972–1974.

Carroll JM, Crompton T, Seery JP, Watt FM. 1997. Transgenic mice expressing IFN-gamma in the epidermis have eczema, hair hypopigmentation, and hair loss. J Invest Dermatol 108:412–422.

Crotta S, Stilla A, Wack A, D'Andrea A, Nuti S, D'Oro U, Mosca M, Filliponi F, Brunetto RM, Bonino F, Abrignani S, Valiante NM. 2002. Inhibition of natural killer cells through engagement of CD81 by the major hepatitis C virus envelope protein. J Exp Med 195:35–41.

Disson O, Haouzi D, Desagher S, Loesch K, Hahne M, Kremer EJ, Jacquet C, Lemon SM, Hibner U, Lerat H. Impaired clearance of virus-infected hepatocytes in transgenic mice expressing the hepatitis C virus polyprotein. Gastroenterology 2004. 126:859–872.

Dolganiuc A, Oak S, Kodys K, Golenbock DT, Finberg RW, Kurt-Jones E, Szabo G. 2004. Hepatitis C core and nonstructural 3 proteins trigger toll-like receptor 2-mediated pathways and inflammatory activation. Gastroenterology 127:1513–1524.

Duncan GS, Mittrucker HW, Kagi D, Matsuyama T, Mak TW. 1996. The transcription factor interferon regulatory factor-1 is essential for natural killer cell function *in vivo*. J Exp Med 184:2043–2048.

Ebihara T, Shingai M, Matsumoto M, Wakita T, Seya T. 2008. Hepatitis C virus-infected hepatocytes extrinsically modulate dendritic cell maturation to activate T cells and natural killer cells. Hepatology 48:48–58.

French AR, Yokoyama WM. 2003. Natural killer cells and viral infections. Curr Opin Immunol 15:45–51.

Frese M, Schwarzle V, Barth K, Krieger N, Lohmann V, Mihm S, Haller O, Bartenschlager R. 2002. Interferon-gamma inhibits replication of subgenomic and genomic hepatitis C virus RNAs. Hepatology 35:694–703.

Gerlach JT, Diepolder HM, Zachoval R, Gruener NH, Jung MC, Ulsenheimer A, Schraut WW, Schrirren CA, Waechtler M, Backmund M, Pape GR. 2003. Acute hepatitis C: High rate of both spontaneous and treatment-induced viral clearance. Gastroenterology 125:80–88.

Golden-Mason L, Madrigal-Estebas L, McGrath E, Conroy MJ, Ryan EJ, Hegarty JE, O'Farrelly C, Doherty DG. 2008. Altered natural killer cell subset distributions in resolved and persistent hepatitis C virus infection following single source exposure. Gut 57:1121–1128.

Golden-Mason L, Rosen HR. 2006. Natural killer cells: Primary target for hepatitis C virus immune evasion strategies? Liver Transpl 12:363–372.

Irshad M, Khushboo I, Singh S, Singh S. 2008. Hepatitis C virus (HCV): A review of immunological aspects. Int Rev Immunol 27:497–517.

Kashiwakuma T, Hasegawa A, Kajita T, Takata A, Mori H, Ohta Y, Tanaka E, Kiyosawa K, Tanaka T, Tanaka S, Hattori N, Kohara M. 1996. Detection of hepatitis C virus specific core protein in serum of patients by a sensitive fluorescence enzyme immunoassay (FEIA). J Immunol Methods 190:79–89.

Knapp S, Warshow U, Hegazy D, Brackbury L, Guha IN, Fowell A, Little AM, Alexander GJ, Rosenberg WM, Cramp ME, Khakoo SI. 2009. Consistent beneficial effects of killer cell immunoglobulin-like receptor 2DL3 and group 1 human leukocyte antigen-C following exposure to hepatitis C virus. Hepatology 51:1–8.

Lanford RE, Guerra B, Lee H, Averett DR, Pfeiffer B, Chavez D, Notvall L, Bigger C. 2003. Antiviral effect and virus-host interactions in response to alpha interferon, gamma interferon, poly(i)-poly(c), tumor necrosis factor alpha, and ribavirin in hepatitis C virus subgenomic replicons. J Virol 77:1092–1104.

Liu F, Song Y, Liu D. 1999. Hydrodynamics-based transfection in animals by systemic administration of plasmid DNA. Gene Ther 6:1258–1266.

Lohmann V, Korner F, Koch J, Herian U, Theilmann L, Bartenschlager R. 1999. Replication of subgenomic hepatitis C virus RNAs in a hepatoma cell line. Science 285:110–113.

Machida K, Tsukiyama-Kohara K, Seike E, Tone S, Shibasaki F, Shimizu M, Takahashi H, Funata N, Taya C, Yonekawa H, Kohara M. 2001. Inhibition of cytochrome c release in Fas-mediated signaling pathway in transgenic mice induced to express hepatitis C viral proteins. J Biol Chem 276:12140–12146.

Major ME, Mihalik K, Puig M, Rehermann B, Nascimbeni M, Rice CM, Feinstone SM. 2002. Previously infected and recovered chimpanzees exhibit rapid responses that control hepatitis C virus replication upon rechallenge. J Virol 76:6586–6595.

Matsuyama T, Kimura T, Kitagawa M, Pfeffer K, Kawakami T, Watanabe N, Kundig TM, Amakawa R, Kishihara K, Wakeham A. 1993. Targeted disruption of IRF-1 or IRF-2 results in abnormal type I IFN gene induction and aberrant lymphocyte development. Cell 75:83–97.

Minakuchi Y, Takeshita F, Kosaka N, Sasaki H, Yamamoto Y, Kouno M, Honma K, Nagahara S, Hanai K, Sano A, Kato T, Terada M, Ochiya T. 2004. Atelocollagen-mediated synthetic small interfering RNA delivery for effective gene silencing *in vitro* and *in vivo*. Nucleic Acids Res 32:e109.

Ochiya T, Nagahara S, Sano A, Itoh H, Terada M. 2001. Biomaterials for gene delivery: Atelocollagen-mediated controlled release of molecular medicines. Curr Gene Ther 1:31–52.

Ohteki T, Yoshida H, Matsuyama T, Duncan GS, Mak TW, Ohashi PS. 1998. The transcription factor interferon regulatory factor 1 (IRF-1) is important during the maturation of natural killer 1.1+ T cell receptor-alpha/beta+ (NK1+ T) cells, natural killer cells, and intestinal intraepithelial T cells. J Exp Med 187:967–972.

Su AI, Pezacki JP, Wodicka L, Brideau AD, Supekova L, Thimme R, Wieland S, Jens B, Purcell RH, Schultz PG, Chisari FV. 2002. Genomic analysis of the host response to hepatitis C virus infection. Proc Natl Acad Sci USA 99:15669–15674.

Takaku S, Nakagawa Y, Shimizu M, Norose Y, Maruyama I, Wakita T, Takano T, Kohara M, Takahashi H. 2003. Induction of hepatic injury by hepatitis C virus-specific CD8+ murine cytotoxic T

lymphocytes in transgenic mice expressing the viral structural genes. Biochem Biophys Res Commun 301:330–337.

Tanaka T, Kitamura F, Nagasaka Y, Kuida K, Suwa H, Miyasaka M. 1993. Selective long-term elimination of natural killer cells *in vivo* by an anti-interleukin 2 receptor beta chain monoclonal antibody in mice. J Exp Med 178:1103–1107.

Thimme R, Oldach D, Chang KM, Steiger C, Ray SC, Chisari FV. 2001. Determinants of viral clearance and persistence during acute hepatitis C virus infection. J Exp Med 194:1395–1406.

Thimme R, Bukh J, Spangenberg HC, Wieland S, Pemberton J, Steiger C, Govindarajan S, Purcell RH, Chisari FV. 2002. Viral and immunological determinants of hepatitis C virus clearance, persistence, and disease. Proc Natl Acad Sci USA 99:15661–15668.

Tseng CT, Klimpel GR. 2002. Binding of the hepatitis C virus envelope protein E2 to CD81 inhibits natural killer cell functions. J Exp Med 195:43–49.

Tsukiyama-Kohara K, Tone S, Maruyama I, Inoue K, Katsume A, Nuriya H, Ohmori H, Ohkawa J, Taira K, Hoshikawa Y, Shibasaki F, Reth M, Minatogawa Y, Kohara M. 2004. Activation of the CKI-CDK-Rb-E2F pathway in full genome hepatitis C virus-expressing cells. J Biol Chem 279:14531–14541.

Vidal-Castineira JR, Lopez ZA, Diaz PR, Alonso AR, Martinez BJ, Perez R, Fernandez SJ, Melon S, Prieto J, Rodrigo L, López LC. 2010. Effect of killer immunogloblin-like receptors in the response to combined treatment in patients with chronic hepatitis C virus infection. J Virol 84: 475–481.

Vilasco M, Larrea E, Vitour D, Dabo S, Breiman A, Reqnault B, Riezu JI, Eid P, Prieto J, Meurs EF. 2006. The protein kinase IKKepsilon can inhibit HCV expression independently of IFN and its own expression is downregulated in HCV-infected livers. Hepatology 44:1635–1647.

Wakita T, Taya C, Katsume A, Kato J, Yonekawa H, Kanegae Y, Saito I, Hayashi Y, Koike M, Kohara M. 1998. Efficient conditional transgene expression in hepatitis C virus cDNA transgenic mice mediated by the Cre/loxP system. J Biol Chem 273:9001–9006.

Yoon JC, Shiina M, Ahlenstiel G, Rehermann B. 2008. Natural killer cell function is intact after direct exposure to infectious hepatitis C virions. Hepatology 49:12–21.

Persistent expression of the full genome of hepatitis C virus in B cells induces spontaneous development of B-cell lymphomas in vivo

*Yuri Kasama,[1] *Satoshi Sekiguchi,[2] Makoto Saito,[1] Kousuke Tanaka,[1] Masaaki Satoh,[1] Kazuhiko Kuwahara,[3] Nobuo Sakaguchi,[3] Motohiro Takeya,[4] Yoichi Hiasa,[5] Michinori Kohara,[2] and Kyoko Tsukiyama-Kohara[1]

[1]Department of Experimental Phylaxiology, Faculty of Life Sciences, Kumamoto University, Kumamoto, Japan; [2]Department of Microbiology and Cell Biology, Tokyo Metropolitan Institute of Medical Science, Tokyo, Japan; [3]Department of Immunology, Faculty of Life Sciences, Kumamoto University, Kumamoto, Japan; [4]Department of Cell Pathology, Faculty of Life Sciences, Kumamoto University, Kumamoto, Japan; and [5]Department of Gastroenterology and Metabology, Ehime University Graduate School of Medicine, To-on, Ehime, Japan

Extrahepatic manifestations of hepatitis C virus (HCV) infection occur in 40%-70% of HCV-infected patients. B-cell non-Hodgkin lymphoma is a typical extrahepatic manifestation frequently associated with HCV infection. The mechanism by which HCV infection of B cells leads to lymphoma remains unclear. Here we established HCV transgenic mice that express the full HCV genome in B cells (RzCD19Cre mice) and observed a 25.0% incidence of diffuse large B-cell non-Hodgkin lymphomas (22.2% in males and 29.6% in females) within 600 days after birth. Expression levels of aspartate aminotransferase and alanine aminotransferase, as well as 32 different cytokines, chemokines and growth factors, were examined. The incidence of B-cell lymphoma was significantly correlated with only the level of soluble interleukin-2 receptor α subunit (sIL-2Rα) in RzCD19Cre mouse serum. All RzCD19Cre mice with substantially elevated serum sIL-2Rα levels (> 1000 pg/mL) developed B-cell lymphomas. Moreover, compared with tissues from control animals, the B-cell lymphoma tissues of RzCD19Cre mice expressed significantly higher levels of IL-2Rα. We show that the expression of HCV in B cells promotes non-Hodgkin–type diffuse B-cell lymphoma, and therefore, the RzCD19Cre mouse is a powerful model to study the mechanisms related to the development of HCV-associated B-cell lymphoma. (*Blood*. 2010;116(23):4926-4933)

Introduction

More than 175 million people worldwide are infected with hepatitis C virus (HCV), a positive-strand RNA virus that infects both hepatocytes and peripheral blood mononuclear cells.[1] Chronic HCV infection may lead to hepatitis, liver cirrhosis, hepatocellular carcinomas[2,3] and lymphoproliferative diseases such as B-cell non-Hodgkin lymphoma and mixed-cryoglobulinemia.[1,4-6] B-cell non-Hodgkin lymphoma is a typical extrahepatic manifestation frequently associated with HCV infection[7] with geographic and ethnic variability.[8,9] Based on a meta-analysis, the prevalence of HCV infection in patients with B-cell non-Hodgkin lymphoma is approximately 15%.[8] The HCV envelope protein E2 binds human CD81,[10] a tetraspanin expressed on various cell types including lymphocytes, and activates B-cell proliferation[11]; however, the precise mechanism of disease onset remains unclear. We previously developed a transgenic mouse model that conditionally expresses HCV cDNA (nucleotides 294-3435), including the viral genes that encode the core, E1, E2, and NS2 proteins, using the Cre/*lox*P system (in core~NS2 [CN2] mice).[12,13] The conditional transgene activation of the HCV cDNA (core, E1, E2, and NS2) protects mice from Fas-mediated lethal acute liver failure by inhibiting cytochrome c release from mitochondria.[13] In HCV-infected mice, persistent HCV protein expression is established by targeted disruption of *irf-1*, and high incidences of lymphoproliferative disorders are found in CN2 *irf-1*$^{-/-}$ mice.[14] Infection and replication of HCV also occur in B cells,[15,16] although the direct effects, particularly in vivo, of HCV infection on B cells have not been clarified.

To define the direct effect of HCV infection on B cells in vivo, we crossed transgenic mice with an integrated full-length HCV genome (Rz) under the conditional Cre/*lox*P expression system with mice expressing the Cre enzyme under transcriptional control of the B lineage–restricted gene *CD19*,[17] we addressed the effects of HCV transgene expression in this study.

Methods

Animal experiments

Wild-type (WT), Rz, CD19Cre, RzCD19Cre mice (129/sv, BALB/c, and C57BL/6J mixed background), and MxCre/CN2-29 mice (C57BL/6J background) were maintained in conventional animal housing under specific pathogen-free conditions. All animal experiments were performed according to the guidelines of the Tokyo Metropolitan Institute of Medical Science or the Kumamoto University Subcommittee for Laboratory Animal Care. The protocol was approved by the Institutional Review Boards of both facilities.

Measurements of HCV protein and RNA

Mice were anesthetized and bled, and tissues (spleen, lymph nodes, liver, and tumors) were homogenized in lysis buffer (1% sodium dodecyl sulfate; 0.5% (wt/vol) nonyl phenoxypolyethoxylethanol; 0.15M NaCl; 10 mM

Submitted May 2, 2010; accepted August 13, 2010. Prepublished online as *Blood* First Edition paper, August 23, 2010; DOI 10.1182/blood-2010-05-283358.

*Y.K. and S.S. contributed equally to this work.

The online version of this article contains a data supplement.

The publication costs of this article were defrayed in part by page charge payment. Therefore, and solely to indicate this fact, this article is hereby marked "advertisement" in accordance with 18 USC section 1734.

tris(hydroxymethyl)aminomethane, pH 7.4) using a Dounce homogenizer. The concentration of HCV core protein in tissue lysates was measured using an HCV antigen enzyme-linked immunosorbent assay (ELISA; Ortho).[18] HCV mRNA was isolated by a guanidine thiocyanate protocol using ISOGEN (Nippon Gene) and was detected by reverse transcription polymerase chain reaction (RT-PCR) amplification using primers specific for the 5′ untranslated region of the *HCR6* sequence.[19,20] Reverse transcription was performed using Superscript III reverse transcriptase (Invitrogen) with random primers. PCR primers NCR-F (5′-TTCACGCAGAAAGCGTCTAGCCAT-3′) and NCR-R (5′-TCGTCCTGGCAATTCCGGTGTACT-3′) were used for the first round of HCV cDNA amplification, and the resulting product was used as a template for a second round of amplification using primers NCR-F INNER (5′-TTCCGCAGACCACTATGGCT-3′) and NCR-R INNER (5′-TTCCGCAGACCACTATGGCT-3′).

Collection of serum for chemokine ELISA

Blood samples were collected from the supraorbital veins or by heart puncture of killed mice. Blood samples were centrifuged at 10 000*g* for 15 minutes at 4°C to isolate the serum.[21] Serum concentrations of interleukin (IL)–1α, IL-1β, IL-2, IL-3, IL-4, IL-5, IL-6, IL-9, IL-10, IL-12(p40), IL-12(p70), IL-13, IL-17, Eotaxin, granulocyte colony-stimulating factor (CSF), granulocyte–macrophage–CSF, interferon (IFN)–γ, keratinocyte-derived chemokine (KC), monocyte chemotactic protein-1, macrophage inflammatory protein (MIP)–1α, MIP-1β, Regulated upon Activation, Normal T-cell Expressed, and Secreted, tumor necrosis factor-α, IL-15, fibroblast growth factor-basic, leukemia inhibitory factor, macrophage-CSF, human monokine induced by gamma interferon, MIP-2, platelet-derived growth factorβ, and vascular endothelial growth factor were measured using the Bio-Plex Pro assay (Bio-Rad). Serum soluble IL-2 receptor α (sIL-2Rα) concentrations were determined by ELISA (DuoSet ELISA Development System; R&D Systems). Serum aspartate aminotransferase (AST) and alanine aminotransferase (ALT) activities were determined using a commercially available kit (Transaminase CII test; Wako Pure Chemical Industries).

Histology and immunohistochemical staining

Mouse tissues were fixed with 4% formaldehyde (Mildform 10 N; Wako Pure Chemical Industries), dehydrated with an ethanol series, embedded in paraffin, sectioned (10-μm thick) and stained with hematoxylin and eosin. For tissue immunostaining, paraffin was removed from the sections using xylene following the standard method,[14] and sections were incubated with anti-CD3 or anti-CD45R (Santa Cruz Biotechnology) in phosphate-buffered saline without Ca^{2+} and Mg^{2+} (pH 7.4) but with 5% skim milk. Next, the sections were incubated with biotinylated anti-rat immunoglobulin (Ig)G (1:500), followed by incubation with horseradish peroxidase-conjugated avidin-biotin complex (Dako Corp), and the color reaction was developed using 3,3′-diaminobenzidine. Sections were observed under an optical microscope (Carl Zeiss).

Detection of immunoglobulin gene rearrangements by PCR

Genomic DNA was isolated from tumor tissues, and PCR was performed as described.[22] In brief, PCR reaction conditions were 98°C for 3 minutes; 30 cycles at 98°C for 30 seconds, 60°C for 30 seconds, 72°C for 1.5 minutes, and 72°C for 10 minutes. Mouse Vk genes were amplified using previously described primers.[23] Amplification of mouse Vj genes was performed using Vκcon (5′-GGCTGCAGSTTCAGTGGCAGTGGRTCWGGRAC-3′; R, purine; W, A or T) and Jκ5 (5′-TGCCACGTCAACTGATAATGAGCCCTCTC-3′) as described.[24]

Results

Establishment of transgenic mice with B lineage–restricted HCV gene expression

We defined the direct effect of HCV infection on B cells in vivo by crossing transgenic mice that had an integrated full-length HCV genome (Rz) under the conditional Cre/*lox*P expression system (Figure 1A upper schematic)[12,19,25] with mice that expressed the Cre enzyme under transcriptional control of the B lineage–restricted gene *CD19*[17] (RzCD19Cre; Figure 1A lower schematic). Expression of the HCV transgene in RzCD19Cre mice was confirmed by ELISA (Figure 1B); a substantial level of HCV core protein was detected in the spleen (370.9 ± 10.2 pg/mg total protein), but levels were lower in the liver (0.32 ± 0.03 pg/mg) and plasma (not detectable). RT-PCR analysis of peripheral blood lymphocytes (PBLs) from RzCD19Cre mice indicated the presence of HCV transcripts (Figure 1C). The weights of RzCD19Cre, Rz (with the full HCV genome transgene alone), CD19Cre (with the Cre gene knock-in at the CD19 gene locus) and WT mice were measured weekly for more than 600 days post birth; there were no significant differences between these groups (data not shown; the total number of transgenic and WT mice was approximately 200). The survival rate in each group was also measured for > 600 days (Figure 1D); survival in the female RzCD19Cre group was lower than that of the other groups.

The spontaneous development of B-cell lymphomas in the RzCD19Cre mouse

At 600 days post birth, mice (n = 140) were killed by bleeding under anesthesia, and tissues (spleen, lymph node, liver, and tumors) were excised and examined by hematoxylin and eosin staining (Figure 2A; supplemental Figure 1, available on the *Blood* Web site; see the Supplemental Materials link at the top of the online article). The incidence of B-cell lymphoma in RzCD19Cre mice was 25.0% (22.2% in males and 29.6% in females) and was significantly higher than the incidence in the HCV-negative groups (Table 1). This incidence is significantly higher than those of the other cell-type tumors developed spontaneously in all mouse groups (supplemental Table 1). Because nodular proliferation of CD45R-positive atypical lymphocytes was observed, lymphomas were diagnosed as typical diffuse B-cell non-Hodgkin lymphomas (Figure 2Aiv,vi-vii; supplemental Figure 1B,E,H,M). Mitotic cells were also positive for CD45R (Figure 2Avi arrowheads). CD3-positive T-lymphocytes were small and had a scattered distribution. Intrahepatic lymphomas had the same immunophenotypic characteristics as B-cell lymphomas (supplemental Figure 1K arrowheads, inset; 1L–N, ID No. 24-4, RzCD19Cre mouse); lymphoma tissues were markedly different compared with the control lymph node (Figure 2Ai,iii,v; ID No. 47-4, CD19Cre mouse) and liver (supplemental Figure 1J; ID No. 24-2, Rz mouse; tissues were from a littermate of the mice used to generate the data in supplemental Figure 1D-I,K-N). All samples were reviewed by at least 2 expert pathologists and classified according to World Health Organization classification.[26] Lymphomas were mostly CD45R positive and located in the mesenteric lymph nodes (Figure 2A; supplemental Figure 1), and some were identified as intrahepatic lymphomas (incidence, 4.2%; supplemental Figure 1K-N). HCV gene expression was detected in all B-cell lymphomas of RzCD19Cre mice (Figure 2B).

To examine the Ig gene configuration in the B-cell lymphomas of the RzCD19Cre mice, genomic DNA was isolated and analyzed by PCR. Ig gene rearrangements were identified in each case (Figure 2C). Genomic DNA isolated from the tumors of a germinal center–associated nuclear protein (GANP) transgenic mouse (GANP Tg#3) yielded a predominant Jk5 PCR product (Figure 2C, Vκ-Jκ); a predominant JH1 product and a minor JH2 product (supplemental Figure 2, DH-JH) were also identified, as previously reported,[22] indicating that the lymphoma cells proliferated from the transformation of an oligo B-cell clone. The B-cell lymphomas of

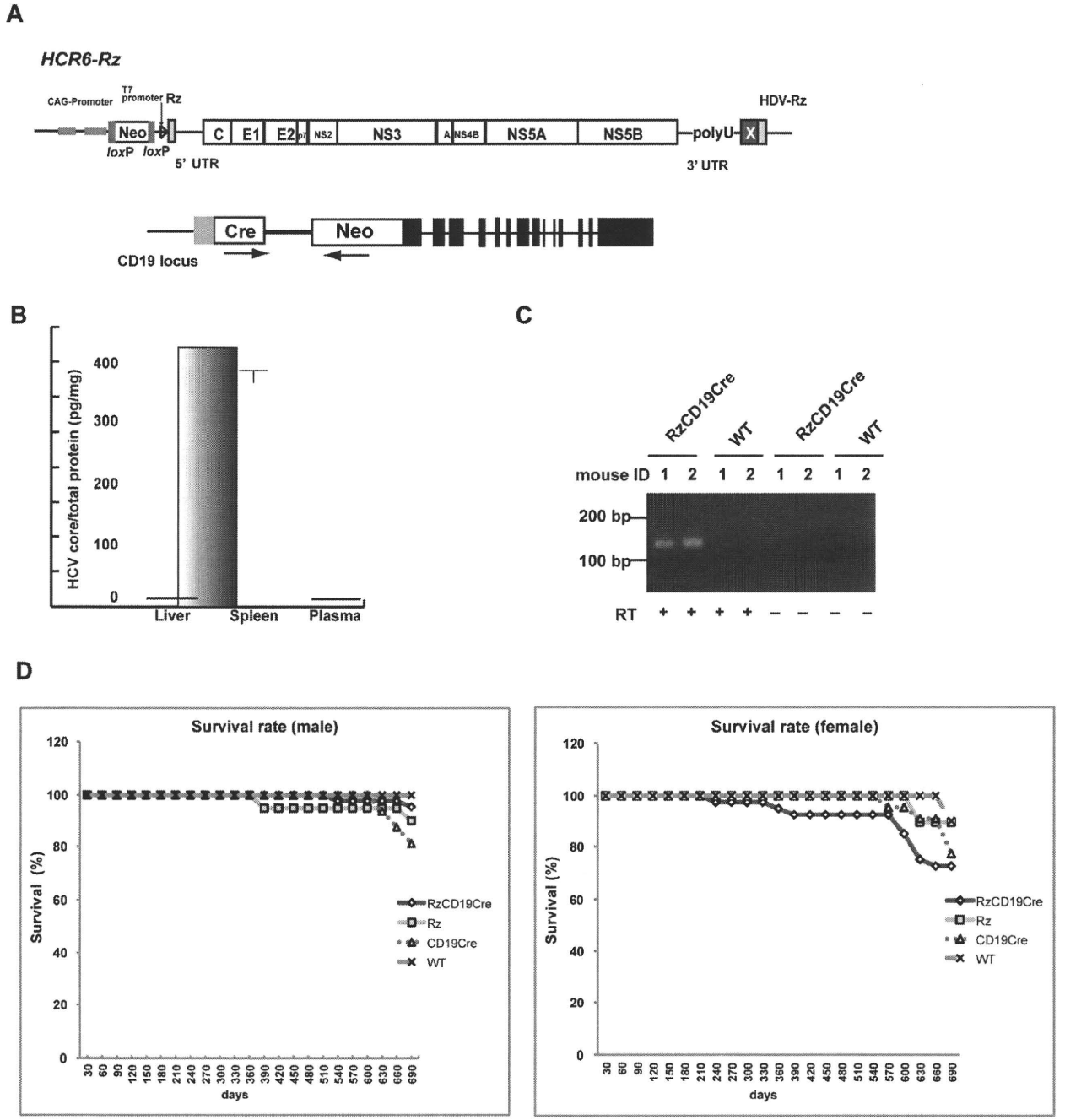

Figure 1. Establishment of RzCD19Cre mice. (A) Schematic diagram of the transgene structure comprising the complete HCV genome (*HCR6-Rz*). HCV genome expression was regulated by the Cre/*lox*P expression cassette (top diagram). The Cre transgene was located in the CD19 locus (bottom diagram). (B) Expression of HCV core protein in the liver, spleen, and plasma of RzCD19Cre mice was quantified by core ELISA. Data represent the mean ± SD (n = 3). (C) Detection of HCV RNA in PBLs by RT-PCR. Samples that included the RT reaction are indicated by +, and those that did not include the RT reaction are indicated by –. (D) Survival rates of male and female RzCD19Cre mice (males, n = 45; females, n = 40), Rz mice (males, n = 20; females, n = 19), CD19Cre mice (males, n = 16; females, n = 22), and WT mice (males, n = 5; females, n = 10).

8 RzCD19Cre mice (mouse ID Nos. 24-1, 54-1, 56-5, 69-5, 42-4, 43-4, 36-3 [data not shown] and 62-2 [data not shown]) yielded a Jκ-5 gene amplification product, and the lymphomas from 3 other mice had the alternative gene configurations Jκ-1 (mouse ID No. 31-4), Jκ-2 (mouse ID No. 24-4) and Jκ-3 (mouse ID No. 42-4; Figure 2C). PCR amplification products from the genes JH4 (mouse ID Nos. 24-1, 24-4, 54-1, 43-4, 56-5, 69-5, 62-2 [data not shown], 36-3 [data not shown]), JH1 (mouse ID Nos. 31-4, 42-4) and JH3 (mouse ID Nos. 31-4, 42-4, 56-5, 43-4, 36-3 [data not shown]) were also detected (supplemental Figure 2). The mutation frequencies in the Jκ-1, -3 and -5 genes were the same as the mutation frequency in the genomic V-region gene.[22] Few or no sequence differences in the variable region were identified among clones from which DNA was amplified. These results indicate the possibility that tumors judged as B-cell lymphomas based on pathology criteria were derived from the transformation of a single germinal center of B-cell origin.

To rule out the oncogenic effect caused by a transgenic integration into a specific genomic locus, we examined if HCV transgene inserted into another genomic site also causes B-cell lymphomas using another HCV transgenic mouse strain, MxCre/CN2-29 (supplemental Figure 3). Expression of the HCV CN2

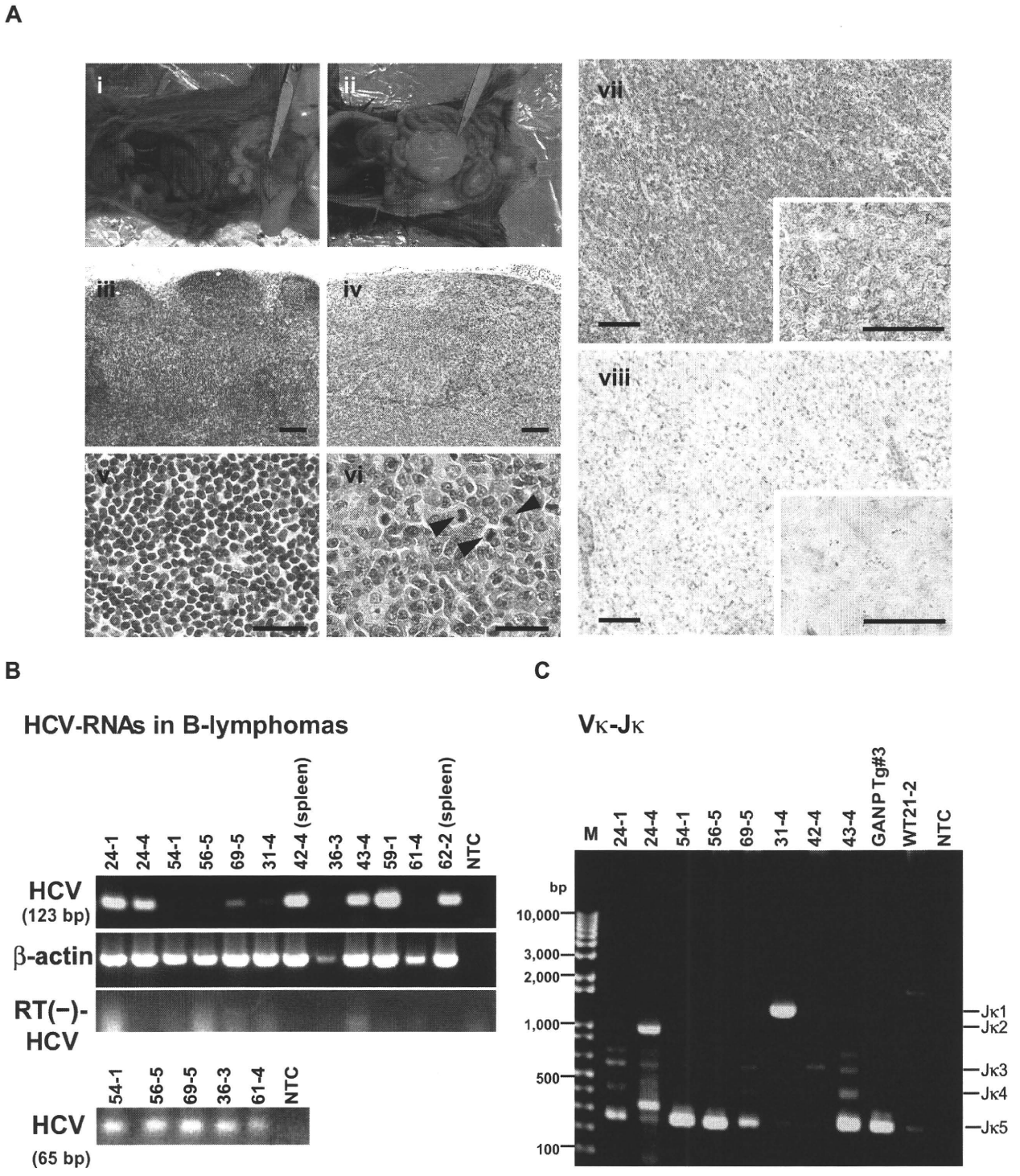

Figure 2. Histopathologic analysis of B-cell lymphomas in RzCD19Cre mouse tissues. (A) Histologic analysis of tissues from a normal mouse (i, iii, v; CD19Cre mouse, ID No. 47-4, male) and a B-cell lymphoma from a RzCD19Cre mouse (ii, iv, vi; ID No. 69-5, male). Paraformaldehyde-fixed and paraffin-embedded tumor tissues were stained with hematoxylin and eosin (iii-vi) or immunostained using anti-CD45R (vii; bottom right, inset) and anti-CD3 (viii; bottom right, inset). Also shown is a macroscopic view of the lymphoma from a mesenchymal lymph node (ii, indicated by forceps), which is not visible in the normal mouse (i). Mitotic cells are indicated with arrowheads (vi). Scale bars: 100 μm (iii-iv, vii-viii) and 20 μm (v-vi, insets in vii-viii). (B) Expression of HCV RNA in B-cell lymphomas from RzCD19Cre mice was examined by RT-PCR. The first round of PCR amplification yielded a 123-base pair fragment of HCV cDNA (upper panel), and a second round of PCR amplification yielded a 65-base pair fragment (lower panel). The β-actin mRNA was a control. As an additional control, the first and second rounds of amplification were performed using samples that had not been subjected to reverse transcription. NTC, no-template control. (C) Ig gene rearrangements in the tumors of RzCD19Cre mice. Genomic DNA isolated from B-cell lymphoma tissues of RzCD19Cre mice (ID Nos. 24-1, 24-4, 54-1, 56-5, 69-5, 31-4, 42-4, 43-4) and spleen tissues of a WT mouse (ID No. 21-2) was PCR amplified using primers specific for Vκ-Jκ genes. Amplification of controls was performed using genomic DNA isolated from a GANP transgenic mouse (GANP Tg#3) and in the absence of template DNA (no-template control, NTC). M, DNA ladder marker.

gene (nucleotides 294-3435)[12] was induced by the Mx promoter-driven cre recombinase with poly(I:C) induction[14] (supplemental Figure 3A). HCV core proteins were detected in both normal spleen (mouse ID Nos. 2, 3, 4) and intra-splenic B-cell lymphoma tissues